ACS Energy LETTERS

http://pubs.acs.org/journal/aelccp

PERSPECTIVE

Luminescent Nanomaterials for Energy-Efficient Display and Healthcare

Manuel A. Triana, En-Lin Hsiang, Caicai Zhang, Yajie Dong,* and Shin-Tson Wu*

Cite This: *ACS Energy Lett.* 2022, 7, 1001−1020

Read Online

ACCESS | Metrics & More | Article Recommendations

ABSTRACT: **Luminescent quantum dots (QDs) and perovskite nanocrystals (PNCs) are promising, efficient energy converters for advanced displays and light sources. Their widespread applications in the photoluminescence (PL)-based displays have been achieved through color enhancement films and patterned color-converters. Meanwhile, electroluminescence (EL) devices based on QDs and PNCs are still under active development, but emerging applications in the healthcare domains could accelerate their adoption. Herein, we first analyze the QD color-conversion displays guided by state-of-the-art research and then summarize the evolution of in situ strategies to fabricate efficient and stable PNC−polymer composites. Subsequently, we introduce the application of flexible QD light-emitting devices for healthcare as a potential early target market. Remaining challenges and future perspectives of QDs and PNCs as light-converters for PL displays, and of QDs for EL applications in healthcare, are analyzed.**

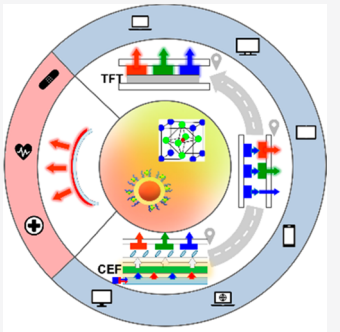

The past decade has seen the establishment of colloidal quantum dots (QDs) as a key element of advanced display technologies[1−5] and the upsurge of perovskite nanocrystals (PNCs) as strong contenders to share the stage with QDs.[6−9] QDs and PNCs both have several desirable properties for photonic and optoelectronic applications, with PNCs attracting an increased interest in the past few years. These PNCs generally have the formula ABX_3, where A is a monovalent cation (Cs^+, $CH_3NH_3^+$ (MA), or $CH(NH_2)_2^+$ (FA)), X a halide anion (Cl^-, Br^-, or I^-), and B a metal cation, typically Pb^{2+}, with its substitution in the PNC structure being a research topic of current relevance due to lead toxicity concerns. Putting them in perspective, both luminescent nanomaterials are considered to have the capability of helping next-generation display technologies to achieve a wide color gamut (WCG) and high energy efficiency simultaneously. These luminescent semiconductor nanomaterials can function in two different energy conversion modes, depending on the excitation mechanism. In the photoluminescence (PL) mode, the emission results after photoexcitation using an external light source with photon energy higher than or equal to the optical bandgap energy ($h\nu \geq E_g^{op}$) of the direct bandgap semiconductor. Meanwhile, in the electroluminescence (EL) mode, the emission originates after electro-excitation by application of an external electric field.

Two main PL applications of the luminescent nanomaterials have been considered for displays to date. The first-generation application of QDs in displays is the use of a color enhancement film (CEF), for which the luminescent nanomaterials are embedded in or coated on a film. Today, the quantum dot enhancement film (QDEF) technology has been widely used for WCG liquid crystal displays (LCDs), achieving over 90% Rec.2020 coverage. The Rec.2020 (also known as BT.2020) is one of the three main color gamut standards, covering the largest area of the visible color space, and has been designed for high-dynamic-range displays. Recently, the

Quantum dots and perovskite nanocrystals both have tunable emission wavelength, high photoluminescence quantum yield (PLQY), and high color purity, with perovskite nanocrystals attracting increased interest in the past few years due to their narrower emission full width at half-maximum, larger absorption coefficient, easier processing, and lower cost.

Received: December 16, 2021
Accepted: February 3, 2022

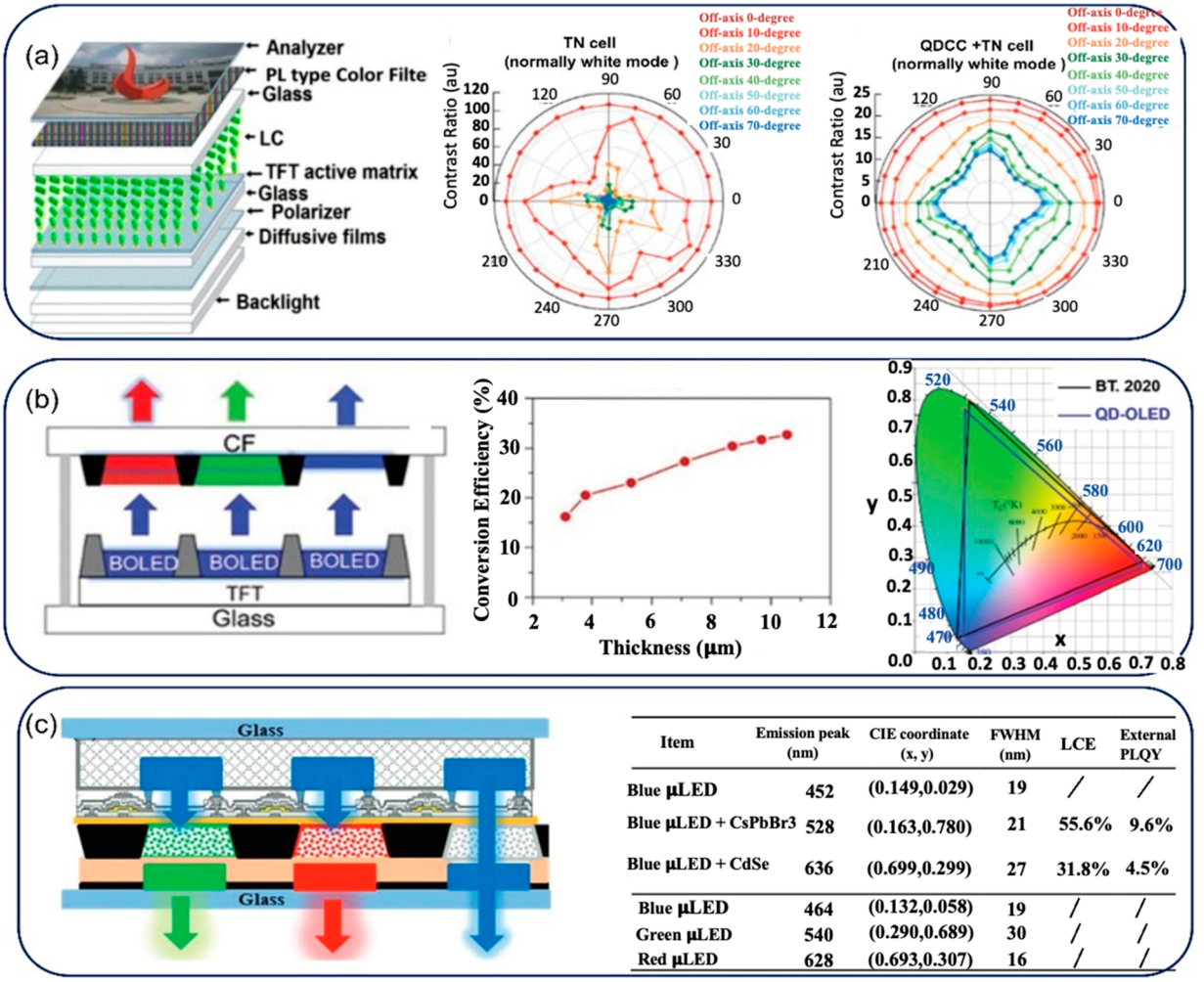

Item	Emission peak (nm)	CIE coordinate (x, y)	FWHM (nm)	LCE	External PLQY
Blue μLED	452	(0.149,0.029)	19	/	/
Blue μLED + CsPbBr3	528	(0.163,0.780)	21	55.6%	9.6%
Blue μLED + CdSe	636	(0.699,0.299)	27	31.8%	4.5%
Blue μLED	464	(0.132,0.058)	19	/	/
Green μLED	540	(0.290,0.689)	30	/	/
Red μLED	628	(0.693,0.307)	16	/	/

Figure 1. Schematic of QDCC enhanced (a) LCDs[29,30] and its viewing angle performance. (b) OLED displays and its color performance. Reproduced with permission from ref 31. Copyright 2020 RSC. (c) Micro-LED display and its color performance.[32] Reproduced with permission from refs 29, 30, and 32. Copyright 2016, 2019, and 2020 Wiley-VCH.

leading QD company, Nanosys, also announced an advanced version of WCG LCDs using the quantum-dot-on-glass technology, which combines the QDEF with a light-guide plate (LGP) by coating QDs directly onto a glass LGP. In contrast to uniformly dispersed QDEF films, the other PL application deposits QD color-conversion materials pixel-by-pixel on top of a blue or UV light excitation source to demonstrate full-color display images. The light source can be an LCD backlight, an organic light-emitting diode (OLED) array, or a micro-light-emitting-diode (micro-LED) array. The displays based on quantum dot color-conversion (QDCC) layers are considered as the second-generation application of QDs. In general, the QDCC technology promises superior performance as compared to the QDEF, with enhanced features such as wider color gamut, wider viewing angle, thinner form factor, lower manufacturing cost, and higher device energy efficiency. The three main display technologies that can benefit from QDCCs and their respective challenges will be discussed in detail in the section Emerging QDCC Technology beyond QDEF.

PNC developments are following the footsteps of QDs, with perovskite color enhancement films (PCEFs) as the initial target and patterned color-converter layers as the immediate next step. The outstanding green emission of PNCs renders them unique opportunities for potential hybridization with QDs or even narrow-band phosphors, while instability remains the biggest challenge to overcome. Importantly, the development of in situ strategies, in particular a swelling−deswelling microencapsulation (SDM) approach, shows the potential of stabilizing PNCs for both the CEF and the color-converter layer technologies, as will be highlighted in the section Perovskite−Polymer Composites for Photoluminescence Applications in Display. Subsequently, current challenges and future directions for the implementation and further penetration of both QDs and PNCs in the display market are summarized in the section Perspective on Quantum Dots- and Perovskite Nanocrystals-Based Photoluminescence for Display.

The EL devices made from QDs (also known as quantum dot light-emitting diodes, QLEDs) or PNCs are often considered as the third-generation display technology and could bring in additional benefits such as printable, ultra-thin, flexible form factors besides the color and efficiency advantages. Pixelated displays using transfer-printed QDs and red/green/blue (RGB) QLEDs driven by an active matrix were first prototyped by Samsung in 2011.[10] Recently, BOE launched a 55-in. QLED display demo featuring a resolution of 3840×2160 and over 90% Rec.2020 color gamut coverage,

https://doi.org/10.1021/acsenergylett.1c02745
ACS Energy Lett. 2022, 7, 1001−1020

representing a breakthrough with respect to previous demos.[11] However, for the industry and the academy in general, there are important challenges to overcome for the full realization of full-color QLED displays, and current efforts are focused on single-color Cd-free QD devices[12−16] and the development and optimization of RGB color patterning.[17−19] The progress status in the optimization of individual LEDs and the race for full-color displays have been extensively reviewed elsewhere for both QDs[3,20,21] and PNCs.[22−24] Meanwhile, research on applications of QLEDs beyond display, such as lighting for healthcare, has been steadily increasing. In this context, our group proposed for the first time the use of flexible QLEDs as wearable photomedical light sources with ideal characteristics for the widespread adoption of phototherapies.[25−27] Flexible QLEDs have desirable properties that can overcome the main limitations of LED- and laser-based phototherapies currently used in clinical settings. Current challenges to advance the application of flexible QLEDs in this area are related to applying thermal management for operation at high brightness (i.e., at high current density) and to improving the encapsulation method for better stability of the devices in air environment. Progresses in these areas and the remaining challenges will be discussed in detail in the section Lighting for Healthcare: Quantum Dot Light-Emitting Diode-Based Photomedicine and thereafter.

EMERGING QUANTUM DOT COLOR-CONVERSION TECHNOLOGY BEYOND QUANTUM DOT ENHANCEMENT FILMS

The first successful application of QDs in display was the PL CEF. Compared to an LCD using a white-LED backlight unit, QD materials, with a narrower emission spectrum than those of two-color phosphors, significantly widen the color gamut by integrating a CEF in the LCD backlight unit. In addition to better color saturation, another factor leading to the success of QDEF is its compatibility with standard LCD manufacturing processes. Because CEFs are placed in front of or onto the LGP with minimal modification to standard LCDs, these technologies can be considered easy drop-in "on-surface" replacements and are thus widely adopted by virtually all major display manufacturers. When a CEF is embedded in the LCD backlight system, the QD material is evenly distributed in the film to convert the blue excitation light to white light. In other words, a portion of the blue light is absorbed by the QD material to generate green and red colors, while the rest is transmitted. A proper mixing ratio of the R/G/B lights forms white light. However, to display full-color images, such a CEF-based system still requires RGB color filters. As a result, nearly two-thirds of the incident white light is absorbed by the color filter in each sub-pixel, leading to a relatively low optical efficiency. In addition, the effect of color filter crosstalk also limits the color performance of the display system. Additional complicated optical structure consists of a functional reflective polarizer, and a patterned half-waveplate is required to further expand the color gamut coverage to over 95% Rec.2020.[28]

Recently, the integration of color-converters was proposed to overcome the limitations of the first-generation QD-CEF technology and further improve the color volume performance of major display technologies using blue backlight, including LCDs, OLED displays, and micro-LED displays. To reduce the absorption loss of color filters and widen the color gamut, a novel QDCC with patterned QD sub-pixels has been proposed to convert the incident excitation blue light in R/G/B sub-pixels into the corresponding R/G/B light. Therefore, compared to conventional QDEFs that produce uniformly distributed white light before reaching R/G/B color filters, the new QDCC not only significantly reduces the absorption loss but also mitigates the crosstalk of color filters. This new QDCC technology is compatible with major display technologies including LCDs, OLED displays, and micro-LED displays, providing better display performances. In the following, we will discuss the advantages and challenges of applying such a QDCC in major display technologies one by one. To enhance light efficiency, the new type of QDCC layer shown in Figure 1a is proposed,[29] which has patterned QD sub-pixels to convert the incident violet (∼410 nm) backlight into the corresponding R/G/B colors. In this device configuration, the liquid crystal (LC) layer only needs to control the gray levels of the deep blue backlight. Thus, a thinner LC layer can be used, which leads to a faster response time.[29] A fast motion picture response time is essential to eliminate image blurs, which is particularly desirable in VR headsets and gaming monitors. Moreover, since the LC layer only modulates a narrowband deep blue backlight, the dark-state light leakage caused by the dispersion of LC material can be minimized, resulting in a higher contrast ratio.

The integration of color-converters was proposed to overcome the limitations of the first-generation quantum dots−color enhancement film technology and further improve the color volume performance of major display technologies using blue backlight.

Furthermore, as shown in Figure 1a, the viewing angle of a twisted nematic (TN) LCD is significantly broadened, benefiting from the isotropic emission of QDs. In contrast to the display using a 450 nm blue backlight with an RG color-conversion layer, Yang et al.[29] proposed to use a violet backlight (410 nm) with an RGB color-conversion layer that provides matched radiation patterns for the RGB sub-pixels to significantly reduce the angular color shift. Otherwise, if a blue backlight is employed, additional scattering particles are required to expand the radiation pattern of blue sub-pixels to match the isotropic emission of QDs in the RG sub-pixels. From the optical efficiency viewpoint, a larger color-conversion efficiency (CCE) in RG sub-pixels can be expected because the QDs exhibit a higher absorption coefficient under a shorter excitation wavelength. However, the low PLQY of blue QDs should be further analyzed. The stability of an LCD panel is governed by two factors: LC material and alignment layer. The absorption of a LC material depends on the conjugation length of the LC compounds, which in turn affects the birefringence. In most LCDs, the employed birefringence is below 0.1 so that its resonance absorption wavelength is shorter than 300 nm. Therefore, the stability of LC material at 410 nm should be robust. The concern is on the long-term stability of the organic alignment layer. For the LCDs requiring a high brightness, inorganic alignment layer, such as SiO_2, is commonly used.

Such a QDCC layer can also be applied to emissive OLED and micro-LED displays, in which the pixelated blue OLED and micro-LED chips are used as light sources to excite the patterned QDs. Such an active-matrix display panel usually

https://doi.org/10.1021/acsenergylett.1c02745
ACS Energy Lett. 2022, 7, 1001−1020

consists of two substrates: the bottom substrate contains millions of thin-film transistors to drive the blue OLED and micro-LED pixels, and the top substrate contains color filters and patterned QDCC. The blue light brightness of each sub-pixel is directly modulated by the thin-film transistors to generate different gray levels. As mentioned above, the patterned QD sub-pixel converts the blue light from OLED or micro-LED to green or red light, and the color filters absorb the leaked blue light from the QDCC, which in turn improves the color purity of the display system. Afterward, these two substrates are aligned and then sealed to form the display module. The integration of QDCCs into these self-emissive displays has aroused great interest in recent years. The benefits of QDCC in each display system are analyzed as follows.

For OLED devices used as excitation sources for QDCCs, sophisticated OLED emitter and device designs are critical to achieve high efficiency and acceptable lifetime. From the perspective of display efficiency, it consists of two parts: (1) the OLED device efficiency, and (2) the QDCC efficiency, which converts the emitted blue light to RG light. Generally, QDCCs have a larger absorption coefficient and higher CCE for a shorter excitation wavelength. Therefore, to enhance the efficiency, the blue OLED devices should fulfill high efficiency and pure-blue or even deep-blue emission spectrum simultaneously. It is known that both emitter design and driving current density affect an OLED's lifetime. The traditional blue fluorescence emitters show reasonable lifetime, so it is widely used in commercial OLED displays. However, its internal quantum efficiency is limited to 25%. On the other hand, although phosphorescent emitters could achieve 100% internal quantum efficiency, the short operational lifetime and sky-blue emission spectrum of blue OLEDs limits its widespread applications. Therefore, phosphorescent emitters have inadequate lifetime, and their sky-blue emission spectrum is not suitable to serve as an excitation light source for QDCCs. It is worth noting that other new blue OLED devices, such as thermally activated delayed fluorescence and hyperfluorescence OLEDs, may also suffer from insufficient lifetime like phosphorescent emitters.[33] Consequently, how to improve the efficiency of blue fluorescent emitters becomes a critical issue. To achieve this goal, the triplet−triplet annihilation OLED device is proposed, which can fuse back the two triplets to singlet through the triplet fusion process. As a result, its internal quantum efficiency can be improved to 65%. Moreover, tandem OLED structure helps to extend the lifetime (e.g., single-layer OLED: n = 1.13; tandem two-layer OLED: n = 1.3; where the value of n is defined by $LT95 \times L0^n$ = constant), and to achieve a higher efficiency (single OLED: 35 cd/A; tandem OLED: 65 cd/A at 300 nits).[34]

Moreover, by using a single-color OLED device, the color variation caused by differential aging of RGB OLED materials can be suppressed. In addition, compared to the RGB OLED display, which suffers from angular color shift caused by the microcavity effect,[35] the isotropic emission of QDCCs significantly expands the viewing angle without noticeable color shift. As a result, as Figure 1b depicts,[31] a tandem blue OLED with QDCCs can achieve ∼95% color gamut in Rec.2020 color space with an improved lifetime, and the luminance conversion efficiency of the QDCC is increased to about 90% for a 10-μm-thick green QD film and about 32% for a 10-μm-thick red QD film.

Another efficient blue light source is micro-LED. To achieve full-color, one can laminate a QDCC layer onto the blue micro-LED array, as Figure 1c (upper part) depicts.[32] Compared to the mass transfer process that transfers RGB micro-LED chips from the fabrication wafers to a display substrate, which has a limited resolution density (normally <1500 pixels per inch, ppi), the color-converted micro-LED display can achieve a higher pixel density (∼3000 ppi) through the wafer bonding process.[36] In addition, as shown in the lower part of Figure 1c, the color-converted micro-LED display exhibits a wider color gamut (∼97% Rec.2020) than that of a RGB micro-LED display (∼75−80% Rec.2020) because the green LED has a broader emission spectrum (∼40 nm). However, as shown in Figure 1c, the external PLQY is very limited, about 10% for green light and 5% for red light. The loss mechanism and improvement method of the QDCC layer will be discussed later. In addition to resolution density, color-converted micro-LED displays helps reduce the complexity of display driver circuits. For RGB micro-LED displays, the wavelength shift caused by the bias voltage and different driving current range between RGB LED chips places a heavy burden on the circuit design. In addition to wavelength shift, the radiation pattern mismatch between the RGB micro-LEDs can also cause a noticeable angular color shift. This radiation pattern mismatch may also occur in color-converting micro-LED displays, if the scattering particles cannot expand the angular distribution of blue sub-pixels to match with that of RG sub-pixels. Furthermore, the high-yield mass transfer and mass repair techniques are still under active development. Before the cost reaches a comparable level with LCDs and OLEDs, the major application of micro-LED displays is likely to aim at high-end products.

In addition, for a high ppi display, e.g., the LED chip size is 8 μm, the color-converted micro-LED display is expected to have a higher power efficiency than the RGB micro-LED display due to the relatively low efficiency of InGaP-based red LEDs, especially when the chip size is small. In comparison with GaN-based blue LEDs, the severe internal quantum efficiency degradation of red micro-LEDs is attributed to the faster surface recombination rate of InGaP semiconductor materials. Therefore, if the photon-conversion efficiency of the QDCC is kept at 33%[37] and the blue GaN LED efficiency is more than 3 times that of the InGaP red LED, then the efficiency of the color-converted micro-LED display will be better than that of RGB micro-LED display. Here, photon-conversion efficiency is defined as the ratio of the photons emitted by the luminescent material to the total incident photons. As shown by Li et al.,[38] and based on the ABC model,[39] when the LED chip size is smaller than 30 μm, the internal quantum efficiency of GaN blue LEDs is more than 3 times that of InGaP red LEDs. Although a specially designed InGaN-based red LED with relatively high external quantum efficiency (EQE ≈ 9.2%) has been demonstrated, the general efficiency of InGaN-based red micro-LEDs is still limited. Extensive research on developing suitable epitaxy and doping methods is still in progress.[40,41]

Although the concept of QDCC is intuitive, several challenges remain to be overcome. The first is to pattern RGB QD arrays on a high-resolution density (∼2000 ppi) display panel with good uniformity. Photolithography and inkjet printing are the two main patterning techniques. Each approach has its own pros and cons. For instance, inkjet printing directly prints QD patterns in the target area and offers on-demand jetting to avoid material waste, while photolithography is a fast-manufacturing process with controllable thickness and is compatible with state-of-the-art facilities

https://doi.org/10.1021/acsenergylett.1c02745
ACS Energy Lett. 2022, 7, 1001−1020

in the semiconductor industry. However, high resolution is difficult to achieve with inkjet printing, and QDs need high resistance in photolithography due to the additives and harsh conditions during the processing. In addition to QD patterning with high-resolution density, another important challenge is the QDCC efficiency. There are several factors limiting the overall efficiency of the QDCC layer. In contrast to QDEF employed in LCD backlight systems which only needs to partially convert the blue LED light to RG colors using a ∼100-μm-thick film with QD concentration <1%, QDCC aims to completely absorb and efficiently convert the incoming blue light to the desired green or red light using a QD film of about ∼10 μm. Thus, a high QD loading is required in the QDCCs. However, the high concentration QD-polymer composite film aggravates the QD reabsorption, Forster resonance energy transfer (FRET), and aggregation caused by phase separation of QD and polymer composites. As a result, decreased PL efficiency, shifted emission peak, and expanded emission bandwidth can be observed.[42−47] As indicated before,[48] compared to liquid-state QDs, the quantum efficiency of high concentration solid-state films drops significantly according to the mechanisms mentioned above. To improve the efficiency of high concentration QDs in the polymer matrix, Kim et al. successfully dispersed QDs in a photoresist film with QD loading up to 30 wt% and achieve 40% quantum efficiency.[49] Note that quantum efficiency is the ratio of the number of photons emitted from a film to the number of photons absorbed by the film. However, the important lifetime issue of the QD film is not discussed by Kim et al.[49] Furthermore, the ligand exchange[50−52] plays an important role to disperse QDs in the host material for improving the stability and efficiency of such a high-concentration QD film. As previously shown,[53] through the ligand exchange and sol−gel condensation process, a QD/siloxane ink can be prepared for the patterning process. Compared to conventional QD/photoresist ink, the QD/siloxane shows a superior stability under harsh heat and moisture conditions (85 °C/5% RH and 85 °C/85% RH). Although the stability of QD film is significantly improved, the quantum efficiency of the QD film is still limited to about 40% at 30 wt% QD concentration. A simple fabrication process without QD surface engineering was also discovered to prepare the QD blending, which is further used in the photolithographic patterning process.[54] The nonpolar ligand capped QDs are dispersed in the nonpolar solvent (toluene) and dried to get QD powder. Next, the QD powder is dispersed in PGMEA with dispersants and oligomeric binders (polyether acrylates). Finally, the mixture is further mixed with extra oligomeric binders, cross-linkable monomers, and photo initiators in PGMEA to form photosensitive QD compositions. This simple fabrication process is attractive for mass production, but its quantum efficiency declines from ∼45% to ∼22% during the patterning process. Overall, the PLQY of a high-concentration QD film is still limited to 40−50%. This value is much lower than the PLQY of a low-concentration QD film and of QDs dispersed in solvent.

In addition to quantum efficiency drop, the high-concentration QDCC films still suffer from two optical loss mechanisms: inadequate absorption of the excitation light and low light extraction efficiency of the converted photons. The trapped converted light in the color-conversion layer could be reabsorbed by the QD materials or absorbed by the sidewall bank, which is usually formed between each sub-pixel to prevent color crosstalk,[36,55,56] The severe color crosstalk in the QDCC layer results from its large aspect ratio (the ratio of QDCC's thickness to sub-pixel width). Especially, in a high-resolution-density display, the aspect ratio of the QDCC layer is often close to or even larger than one. Such a large aspect ratio provides space for the excitation light to travel from one sub-pixel to cross-excite the QD materials in adjacent sub-pixels, resulting in a degraded color purity. However, the absorptive insulating banks also lead to severe light loss and decreased QDCC efficiency. Based on the isotropic emission of QD material and the refractive index difference between QDCC layer and air, only about 20% of the light can be extracted from the top surface, as in OLED devices. Furthermore, to improve color purity and reduce ambient light excitation of QDs, absorptive color filters are commonly used on top of the QDCC layer to absorb the leaked excitation light. It causes an extra 10−20% loss for the converted light. It is also worth noting that the leaked excitation photons are absorbed by the color filters.

Three major approaches have been developed to improve the overall efficiency of the QDCC layer. The first approach is the additive optical film. As shown in Figure 2a, to improve the excitation light absorption, a high-pass filter recycles the blue light leaked from the QDCC back to the film to excite the QD material, and the absorption filters on top of the QDCC prevents blue light leakage and eliminates ambient light excitation.[57,58] The band-pass filter can be a distributed Bragg reflector (DBR) or a stacked cholesteric liquid crystal (CLC) film with opposite chirality.

Moreover, to mitigate the issue of low light extraction efficiency of the converted photons, Figure 2a shows that the short-pass filter below the QDCC reflects the backward QD emission to the upward direction. As illustrated in Figure 2a, the hybrid Bragg reflector (HBR) and DBR can increase the CCE by about 10% and 20%, respectively. In addition, by combining the DBR film and the blue light filter, the blue light leakage is significantly reduced, and the color purity is improved by about 50%.[59] However, at large incident angles, the blue-shift of the reflectance spectrum leads to a decreased reflectivity of DBR films for the designed wavelength. Therefore, under such circumstances, the amount of blue light leakage becomes angle dependent and may affect the color performance at different viewing angles. But this issue may not be too serious because an absorption filter can be further laminated on top of the DBR layers to absorb the leaked blue light without angular dependency. Moreover, the complicated fabrication process and high cost of DBR restricts its wide adoption. Recently, Theobald et al.[60] proposed to use core−shell nanoparticles as a selective reflector to reflect the converted photons to the forward direction and scatter the excitation light simultaneously. Compared to the traditional DBR design, a 4× absorption enhancement and 2× out-coupling efficiency improvement has been achieved. A similar function selective reflector is also demonstrated by Chen et al. based on an Ag/TiO_2 nanocomposite material.[61]

The second approach to boost QDCC efficiency relies on the scattering particles. Unlike traditional luminance material phosphors with diameter about a few microns, the QD nanoparticles exhibit negligible light scattering. Therefore, adding scattering particles in the QDCC layer fulfills this function. Figure 2b illustrates the design principle of scattering particles.[62] As shown in Figure 2b, SiO_2, TiO_2, and ZnO scattering particles, which are widely employed to improve the

https://doi.org/10.1021/acsenergylett.1c02745
ACS Energy Lett. 2022, 7, 1001−1020

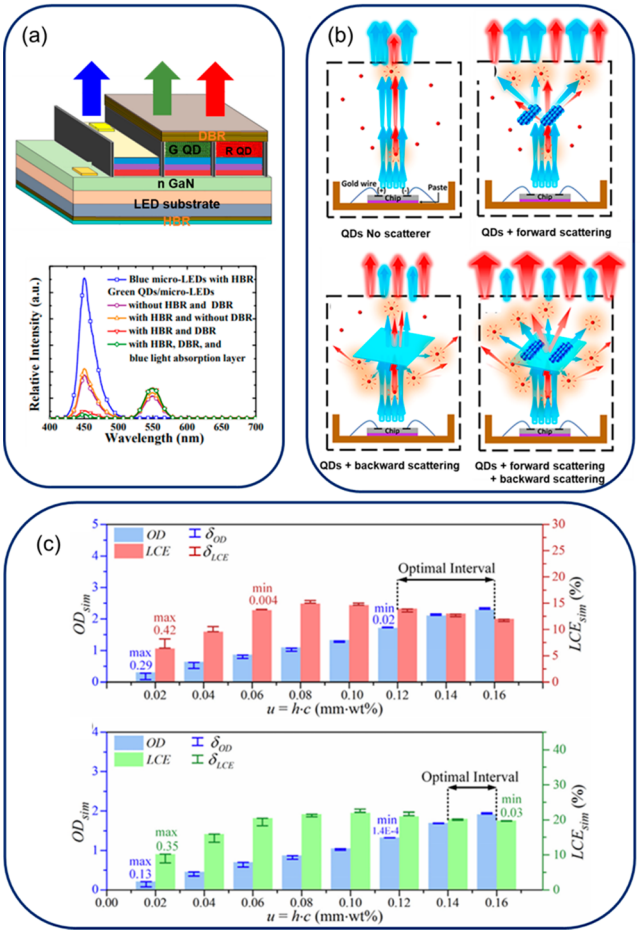

Figure 2. Strategies for enhancing the optical performance of QDCCs. (a) An optical thin film coating (HBR, DBR, and color filter) on a QDCC. Reproduced with permission from ref 57. Copyright 2017 IEEE. (b) Illustration of mixing particles in QD film. Reproduced with permission from ref 62. Copyright 2020 ACS. (c) Optimizing the product of thickness and concentration of the QDCC layers. Reprinted with permission from ref 63. Copyright 2021 The Optical Society.

light extraction efficiency of converted photons through forward scattering, can hardly enhance or even reduce the absorption of excitation light.[64,65] Therefore, the overall light conversion efficiency improvement is still inadequate, and the color purity is also not improved significantly. To absorb more excitation photons, a 2D nanoplate is used to generate backward scattering. Based on the two mechanisms mentioned above, we can summarize that ideal scattering particles should provide not only backward scattering for increasing the absorption of excitation light but also forward scattering for enhancing the light extraction efficiency of the converted photons. Therefore, Gao et al.[62] mixed the 0D SiO_2 scattering particles with 2D boron nitride (BN) nanoplates together and improved the light conversion efficiency by 99%, 13%, and 27% in comparison with pure QDCC, QDCC with 0D SiO_2 only, and QDCC with 2D BN nanoplates only. Scattering effects can also be achieved by the micropores in a polymer matrix, which shows 6.6× PL enhancement.[66] In addition, pore-structured nanoparticles can also be used to reduce the self-absorption of QD materials.[67] The converted light is coupled into the waveguide structure of the nanoparticles, avoiding reabsorption from the QDs present in the pore region.

Other system optimization approaches have also been proposed to optimize the thickness, concentration, and geometry of the QDCC layers to improve the overall display performance. A thicker QDCC layer and higher QD concentration results in a higher absorption of excitation photons and purer colors. However, it also leads to a more severe reabsorption loss in QDs. Therefore, an optical model is established to optimize the QD material concentration and QDCC layer thickness to achieve a proper balance between the absorption of excitation photons and light conversion efficiency.[68,69] As shown in Figure 2c,[63] the optimized dose factor (the product of QDCC layer thickness and QD concentration) should exhibit an OD > 1.7 and a light conversion efficiency >80% of its maximum value. As the dose factor increases, the absorption of blue light increases following the Beer's law, but the light conversion efficiency first increases and then decreases. The declined light conversion efficiency mainly results from the strong self-absorption of high-concentration QD materials. Furthermore, as mentioned above, in the QDCC layer, most of the photons are absorbed by the sidewall insulating banks. Therefore, a new research direction has been recently proposed to implement a reflection−scattering type of insulating bank or to optimize the reflection funnel geometry for improving the overall display efficiency.[70,71] However, the effects of ambient reflection and ambient excitation of the QDCC layer should also be considered when applying such a reflective insulating bank. Considering the ambient light effect, the geometry of the reflective insulating bank can be optimized to achieve 3× efficiency enhancement.[72]

PEROVSKITE−POLYMER COMPOSITES FOR PHOTOLUMINESCENCE APPLICATIONS IN DISPLAY

In the case of PNCs for PL display applications, both CEF and color-conversion approaches have been investigated. Green perovskite films and yellow hybrid perovskite/phosphor films working as perovskite color enhancement films (PCEFs) for simultaneous high brightness and WCG coverage have been proposed by Zhijing Nanotech,[73] Nanolumi, and Avantama. At the CES 2018 conference, TCL in cooperation with Zhijing Nanotech[74] released the first TV prototype with enhanced color gamut and brightness enabled by PCEFs, which were fabricated on a large scale by roll-to-roll processing. Despite the impressive progress, the most critical challenge for practical applications of PNCs is their instability under external stimuli, namely, exposure to heat, light, oxygen, and/or humidity, which demands the development of strategies to effectively protect the PNCs against detrimental effects. Several strategies have been proposed for simultaneous fabrication and encapsulation of PNCs, with in situ fabrication in polymer matrices being the most attractive for early commercialization through perovskite−polymer composites (PPCs). Among these strategies are blended spin-coating, controllable drying, swelling−deswelling microencapsulation (SDM), microfluidic spinning, and in situ polymerization from monomers and perovskite precursors. These strategies have already been reviewed elsewhere.[74] Remarkably, the development of SDM and "controllable drying" strategies to fabricate stable PPCs has opened a unique opportunity to demonstrate the potential of PNCs for PL applications.[73−75] Here, the evolution of the

https://doi.org/10.1021/acsenergylett.1c02745
ACS Energy Lett. 2022, 7, 1001−1020

SDM strategy is reviewed in detail because it is believed to stand out as one promising direction for overcoming the PNCs' instability challenges for both CEF and color-conversion approaches for displays.

The swelling−deswelling microencapsulation strategy is believed to stand out as one promising direction for perovskite nanocrystals research and development, considering its simplicity and versatility for large-scale fabrication of stable perovskite−polymer composites and its potential for realizing both perovskite-based color enhancement films and color-conversion displays.

Essentially, by direct contact of the perovskite precursor solution with cross-linked polymers, the solvent can swell the polymer matrices, and by this swelling process the perovskite precursor and the solvent are introduced into the polymer. Subsequently, the baking of the sample evaporates the solvent and stimulates the formation and growth of the PNCs, while the polymer matrix contracts, forming a barrier layer around the as-synthesized PNCs by the deswelling process (see Figure 3a). This approach was first demonstrated in 2016 using an organic−inorganic perovskite ($MAPbBr_3$, $MA^+ = CH_3NH_3^+$) precursor with dimethylformamide as the solvent and applied in different polymers.[76] By using the same SDM strategy, green-emission $CsPbBr_3$ perovskite nanorods with preferred orientation direction and potential application in LCD backlight units were also developed.[77]

Subsequently, PPCs with emission color over the visible range were obtained by the ligand-assisted SDM strategy (Figure 3b) in order to widen the color gamut for display applications.[78] Importantly, the above SDM strategies could only be applied to polymer films, and a very cost-effective one-step method to synthesize perovskite-on-polymer microspheres with full-color emission and good stability was further developed (Figure 3c) in order to boost the potential application of the SDM approach.[79] Although previous work demonstrated stable, efficient green PPCs, further efforts are still needed to enhance the stability for practical applications, and despite the protection of the above-mentioned polymer matrices, red-emitting $CsPbBr_xI_{3-x}$ PPCs are not as stable as the green PPCs, especially under harsh test conditions. Therefore, an advanced SDM strategy, named the deep-dyeing method was developed to convert highly inert polymer matrices into high-efficiency PPCs with superior stability.[80] By full immersion of the inert solvent-resistant polymer (e.g., polyethylene terephthalate, PET) at a suitable high temperature, the polymer chains were well swelled, allowing the perovskite precursors to enter the interior of the polymer matrix. And after sufficient deswelling, the luminescent deep-dyed PPCs with different form factors were fabricated (see Figure 3d). The as-synthesized deep-dyed PPCs showed excellent PLQY of up to 77.9%, outstanding color purity (full width at half-maximum, fwhm ≈ 18−42 nm), and tunable wavelength from 477 to 645 nm. Also, the obtained deep-dyed PPCs showed magnificent water stability, thermal stability, and photostability due to the robust protection of the PET matrix. Remarkably, this approach further improved the stability of both green and red deep-dyed PPCs, so that they survived in water for years with no signs of degradation. Accordingly, these

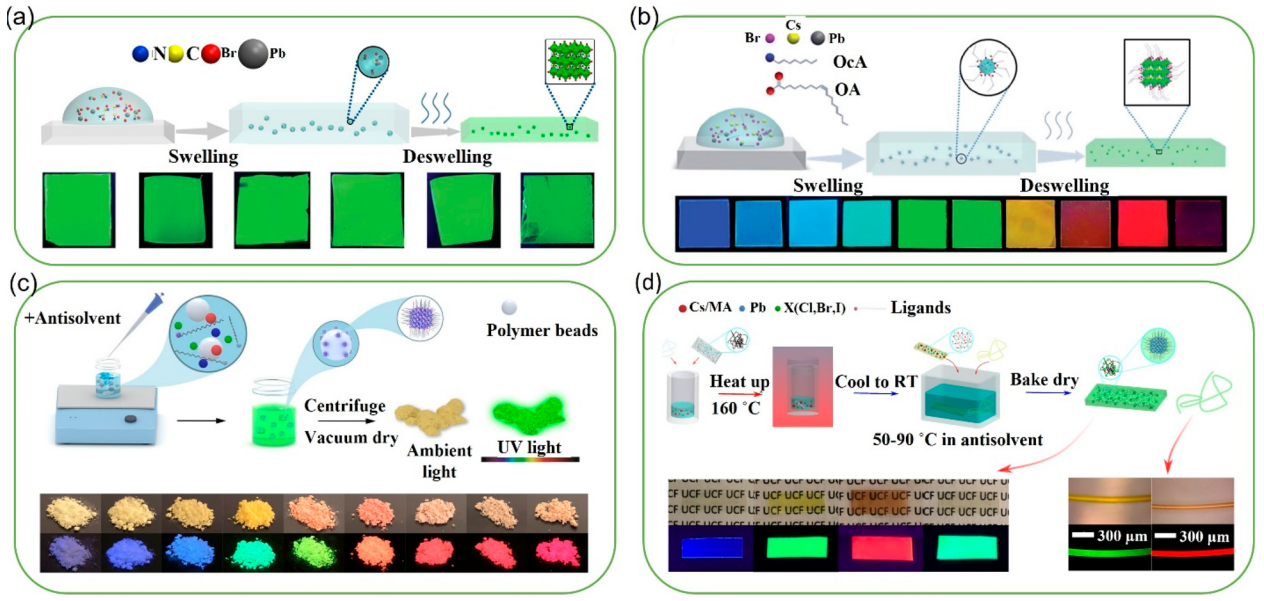

Figure 3. Strategies for the encapsulation of PNCs. (a) Scheme of the PPC film formation by the SDM mechanism. PPCs prepared by spin coating under UV light. Reproduced with permission from ref 76. Copyright 2016 Wiley-VCH. (b) Scheme of the ligand-assisted SDM strategy. Pictures of spin-coated luminescent PPCs.[78] (c) Step-by-step process to fabricate light-diffusing, down-converting, perovskite-on-polymer microspheres. Microspheres with different anion compositions under ambient and UV light.[79] (d) Step-by-step illustration of the deep-dyeing SDM strategy and photos of deep-dyed PPC films and fibers under ambient and UV light.[80] Reproduced with permission from refs 78−80. Copyright 2019, 2020, and 2021 RSC.

https://doi.org/10.1021/acsenergylett.1c02745
ACS Energy Lett. 2022, 7, 1001−1020

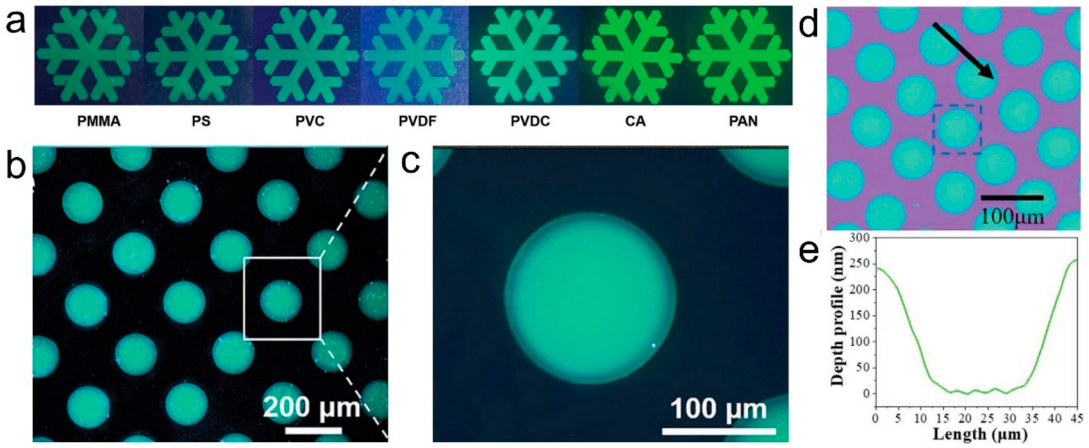

Figure 4. Patterned color-converters fabricated by inkjet printing based on the SDM mechanism. From Zhong's group: (a) optical images of printed perovskite QD patterns on different polymer substrates under UV light and (b, c) microscopic images of a pixels array (b) and a single microdisk (c) in dark field.[81] From Sun's group: (d) microscopic fluorescent image of a large-area picture and (e) depth profile of one single microdot.[82] Reproduced with permission from refs 81 and 82. Copyright 2019 and 2020 Wiley-VCH.

improved deep-dyed PPCs are believed to have great potential as down-converting materials for numerous applications, including LCD backlighting and luminescent textiles.

On the other hand, Zhong's group[81] and Sun's group[82] took advantage of the SDM strategy to perform the patterning of PNCs onto polymeric sheets by in situ inkjet printing. Figure 4a shows the same image printed on different polymer substrates, and Figure 4b,d shows printed arrays with pixel sizes of ∼150 and 65 μm, respectively.

The large-area, highly luminescent (PLQY up to 80%), and color-tunable (400−750 nm) pixel arrays achieved by in situ inkjet printing demonstrate the applicability and versatility of SDM on a variety of polymers, which in turn show high potential for low-cost, simple patterning of PNC color-conversion films soon.

Finally, it is worth mentioning that the PNCs discussed here are all lead halide perovskites, which are superior to any lead-free PNCs reported to date in terms of optical performance. However, the toxicity concerns of lead-based PNCs and the Restriction of Hazardous Substances (RoHS) limit of 1000 ppm for Pb content in electronic devices have stimulated a lot of research on lead-free PNCs in the recent years. In general, different candidates such as Sn^{II}, Sn^{IV}, Sb^{III}, Bi^{III}, Pd^{IV}, Cu^{I}, Cu^{II}, In^{III}, Ag^{I}, Na^{I}, Eu^{II}, and Yb^{II} have been proposed to replace the Pb^{II} in the PNCs, although there are still important challenges to overcome so that lead-free PNCs achieve optical properties comparable to those of their lead-based counterparts.[83,84] Importantly, we believe that simple solution-processing of these new PNCs will also allow the application of the encapsulation strategies discussed here, in order to further enhance the stability of lead-free PNCs.

PERSPECTIVE ON QUANTUM DOTS- AND PEROVSKITE NANOCRYSTALS-BASED PHOTOLUMINESCENCE FOR DISPLAY

QDEF was the first technology to bring QDs into the display market. Since then, this technology has been widely adopted in commercial products, and the application of QDs continues evolving. Current efforts to further improve the QDEF technology are mainly related to offering high CCE while achieving low manufacturing cost. Some methods proposed to this end include integrating microstructures on the QD film,[85] QD-embedded glass fiber-reinforced siloxane mixtures,[86] and the novel QD diffuser plate for LCDs obtained by a three-layer co-extrusion method without expensive barrier films.[87] In this regard, Nanosys recently launched the xQDEF, which is an extruded diffuser plate technology. With these inventions, display manufacturers and component providers of QD-CEF technologies are pointing to access the low-cost mainstream market of TVs and monitors.

Alternatively, QDCC is a promising next step in the QD technology roadmap for display applications. As most recent developments in this area, Samsung started mass production of QD-OLED panels at the end of November 2021 and could release QD-OLED TVs in 2022, which would be the first QDCC-based display products. Meanwhile, the partnership and joint efforts of leading micro-LED and QD companies could accelerate the introduction of QDCC to micro-LED displays in the future. To fully realize this emerging technology, each display still needs specific development. For instance, OLED displays must guarantee blue OLEDs with long lifetime and high efficiency, LCDs require the insertion of an in-cell polarizer due to the light depolarization caused by the QDs, and micro-LED displays need QD patterning with higher resolution due to the smaller sub-pixel size (<10 μm). To date, only the QD-photoresist patterning can enable microdisplay demos with the required resolution (2−4 μm sub-pixels) for AR/VR displays. Thus, the use of inkjet printing or photolithography for the QD patterning will also depend on the display type. Meanwhile, optimizing the QDCCs' optical performance is a common requirement to the above-mentioned three display types, and one key parameter for this optimization is the blue light absorption of the QDCCs. Importantly, while the QDCC thickness must be thin to keep a reasonably small aspect ratio of the pixels, the QD concentration increase can be detrimental for the CCE due to QD aggregation and self-absorption. Therefore, the most reasonable pathway to advance in this matter will be the improvement of existing QDs or the development of new QDs with high blue light absorption. It is also worth noting the urgent need for further research in heavy-metal-free QDs other than In-based QDs, due to the scarcity of In and to the complex core−shell−shell (C/S/S) structure of the In-based QDs, leading to expensive, time-consuming synthesis. In this

https://doi.org/10.1021/acsenergylett.1c02745
ACS Energy Lett. 2022, 7, 1001−1020

regard, recently reported heavy-metal-free green QDs with confidential composition exhibit a higher blue light absorption (98% for a 10-μm film) in comparison to green indium phosphide (InP) QDs.[88]

Meanwhile, as in the case of QDs for display, it is quite likely that PNCs will be introduced and further developed through a similar initial market and technology roadmap, respectively. However, the PNCs' rapid development in the past few years and the recent announcement of prototype perovskite products are pointing to a faster commercialization pace in comparison to QDs, specifically to CdSe QDs. In 2017, our group[75] proposed an ultra-stable, high-luminescence green PPC film achieved by the SDM strategy as a PCEF, with advantages such as lower cost and higher brightness as compared to the QDEF technology based on InP and CdSe QDs.[89] Accordingly, we proved that high light efficiency (20 lm/W) and wide color coverage (89% Rec.2020) could be achieved at a low cost by "on-surface" integration of the green PCEF with an on-chip red-emitting $K_2SiF_6:Mn^{4+}$ phosphor in the LCD backlight. Since then, several companies have announced PCEF prototypes with performances approaching those efficiency and color gamut targets. The application of PNCs as emerging color-converters is also very promising. In particular, the new green PNCs with an extra narrow emission fwhm (~18 nm) and higher blue light absorption (OD > 2.3) can be an excellent alternative to advance the color-conversion display development by offering improved CCE and wider color gamut. Due to the greater absorption efficiency of PNCs, the material volume loading required for Cd-free PNCs to reach an OD ≈ 2 is about one-third to one-fourth that of InP QDs with a transparent ZnS shell.[90] Both inkjet printing[91] and photolithography[92] have been proven effective to pattern perovskite color-converters with high resolution; furthermore, we expect to see the demonstration of patterned perovskite color-converters with a long lifetime in the near future, since this is a key factor to boost their applications. We can conclude that the similar tunable emission wavelength and high PLQY, plus the easier and lower-cost processing, the narrower emission fwhm, and the higher absorption coefficient of PNCs compared to QDs, promise a bright future for the PL displays of PNCs, which may partially or completely replace QDs in CEFs and beyond.

STATUS OF QUANTUM DOT LIGHT-EMITTING DIODES IN DISPLAY AND EMERGING APPLICATIONS

It is worth noting that the research for display applications has been the main driving force pushing forward the development of QLEDs for more than 20 years. QLEDs development has reached far since they were first introduced, but important challenges remain before their commercialization. The active-matrix (AM) QLED is currently the most suitable technology for full-color electroluminescent QLED displays, which has been adapted from the active-matrix organic light-emitting diode (AMOLED) and micro-LED displays. An AMQLED consists of an active matrix of RGB QLED pixels integrated onto a thin-film transistor (TFT) array, which control the current flow through each individual pixel. Thus, the AMQLED technology results in reduced power consumption and fast response time as compared to the passive-matrix technology, which requires high current densities. By developing this technology, AMQLED displays will share important advantages with AMOLED displays such as light, rigid or flexible, thin form factors, and low power consumption. Furthermore, the capability of AMQLED displays for solution-processed fabrication can make them less expensive than AMOLEDs, which require vacuum evaporation for all the functional layers. In Figure 5, we illustrate the structure of an

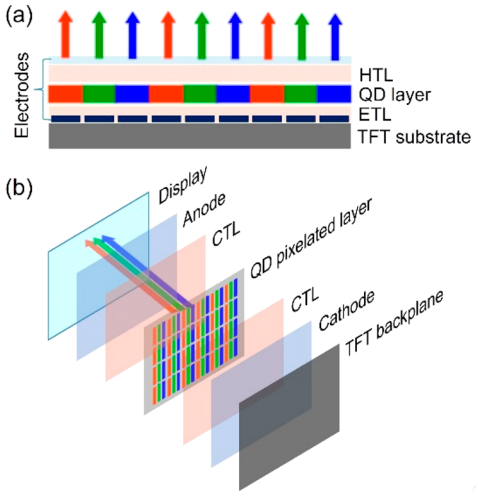

Figure 5. (a) Cross-sectional scheme and (b) expanded structure of an AMQLED display. CTL, charge transport layer; HTL, hole transport layer; ETL, electron transport layer.

AMQLED display using QLEDs with top emission and inverted structure, which are believed to offer more advantages with respect to QLEDs with forward (regular) structure. An inverted structure enables a reverse injection scheme in which holes and electrons are injected from the top anode and bottom cathode, respectively.

There are two main challenging directions under research for the realization of efficient and high-resolution QLED full-color displays. One is the development of single-color QLEDs with simultaneous high efficiency, high brightness, and long lifetime, and the second is the assembly of the AMQLED, in particular, the development of the patterning technique for the RGB QD pixel arrays. To date, the external quantum efficiency (EQE) of all red, green, and blue Cd-based QLEDs has approached the theoretical limit of ~20% (without light outcoupling),[93−96] which is comparable to that of state-of-the-art OLEDs. In addition, green and red on-glass devices have already overcome the commercialization requirement for low- and high-brightness (outdoors) display in Cd-based QLEDs.[96−98] The simultaneous high brightness ($\geq 10^4$ cd m^{-2}) and EQE (≥20%) achieved for all red, green, and blue QLEDs are also promising developments for lighting applications.[12,14,93,94,96,99] In addition to the efforts for further improvement of the efficiency, brightness, and operating lifetime, other current developments are focused on the design of flexible QLEDs with multiple form-factors, the substitution of Cd-based QDs in the devices, and the reduction of fabrication costs. For instance, red[12,16] and blue[14] Cd-free QLEDs using InP/ZnSe/ZnS and ZnTeSe/ZnSe/ZnS C/S/S QDs, which exhibited maximum EQE values above 20% and half lifetimes of 1×10^6 and 1.58×10^4 h, respectively, were recently reported. Further improvements of the operating lifetime in individual blue QLEDs[95,98] and the performance in green InP-based QLEDs are needed.[100] Recent research has demonstrated that thorough tailoring of the InP-based C/S/S QDs structure, ligand passivation, and interfacial engineering

https://doi.org/10.1021/acsenergylett.1c02745
ACS Energy Lett. 2022, 7, 1001−1020

are key directions to avoid accelerated degradation and achieve highly stable, efficient green and blue QLEDs.[13,15]

On the other hand, regardless of the advances in the performance of single-color QLEDs, their full-color displays still seem some miles away from full realization. An important challenge in this direction is the development of a patterning technique that can guarantee simultaneous high-efficiency and high-resolution full-color QLED displays. Ongoing research has been focused on optimizing existing techniques used for patterning of the RGB QD pixel arrays. For instance, other kind of inkjet printing called electrohydrodynamic jet printing[18] was developed to produce high-resolution QD patterns and pixelated QLEDs. A technique called direct optical lithography of functional inorganic nanomaterials (DOLFIN)[19] was developed to replace organic photoresist with photosensitive inorganic ligands. Furthermore, intaglio transfer printing[17] has been proposed as a promising pathway for integrating high-definition full-color displays to wearable electronics. In our view, each of the existing techniques has important "pros and cons". For instance, inkjet printing offers on-demand jetting to avoid material waste, and photolithography is compatible with state-of-the-art facilities already in the semiconductor industry. However, high resolution is difficult to achieve with inkjet printing, and both charge transport materials (metal oxide and organic materials) and QDs need high chemical resistance in photolithography due to the additives and harsh conditions during processing. On the other hand, transfer printing is a solvent-free technique, but scaling up is difficult, and multiple use of the stamps (e.g., PDMS) can lead to wear-out and subsequent pixel defects. Further improvements or developments of novel approaches are needed, and cost-effective techniques that are compatible with state-of-the-art facilities can pay off in this race.

Today, QLED is a growing technology regardless of the remaining challenges for commercial applications, and development efforts on new features of QLEDs such as light weight, thinness, and flexible form-factors have opened up opportunities for other applications, beyond displays. Research papers addressing alternative applications of QLEDs such as wearable devices for photomedicine, diagnostics, and health monitoring have steadily increased since 2005, according to data from Web of Science searches represented in the bar chart in Figure 6. Briefly, we first collected the papers reported on QLEDs by searching for all the possible variations referring to QLEDs within the topic of the papers. Then, the QLED papers addressing applications such as photomedicine, biomedicine, biosensing, optical communication, etc., were recovered, while the QLED papers specifically related to the display field were excluded. As observed, the volume of papers on applications different than display is expected to increase as the research on QLEDs also increases, indicating the interest of researchers in exploring alternative applications for QLEDs in the past 15 years.

Particularly, the development of wearable devices is pushing forward the application limits of QLEDs, as they are the QD-based devices most frequently integrated into wearable systems under research. We consider that the research on QLEDs as wearable light sources in the healthcare field can push forward the application of electroluminescent QLED devices, given the simpler design of this technology and multiple other benefits. Accordingly, the following sections are dedicated to explaining in detail the potential, progress, and future perspectives for the application of QLEDs as wearable light sources in the

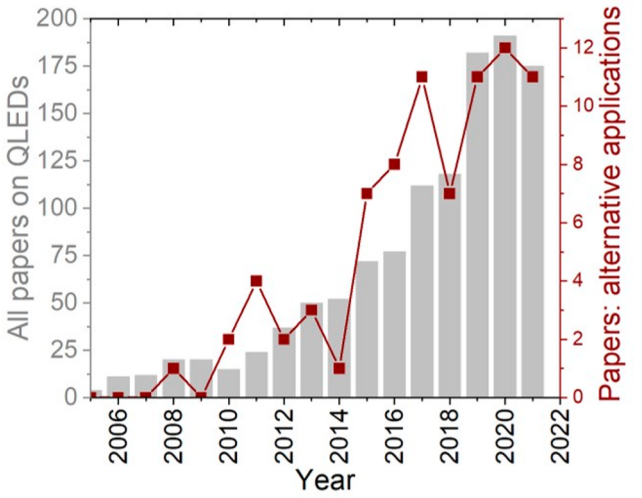

Figure 6. Number of QLED papers and the corresponding QLED papers on applications alternative to display from 2005 to 2021, based on the Web of Science.

photomedicine field. It is worth noting that, although QLEDs emitting at different wavelengths across the visible spectrum (including the near-infrared) could find an application in the vast field of photomedicine, the red and deep-red emission wavelengths are of high clinical relevance for diagnosis and therapy.[101,102] Importantly, red light penetrates the biological tissue deeper than the green and blue light, and still has enough energy to promote cell proliferation or excite substances called photosensitizers for the application of different phototherapies. In addition, red QLEDs are the most well developed single-color QLEDs with clear and proved advantages compared with red OLEDs. Therefore, the following sections will focus on the development of red-emitting QLED devices for healthcare.

LIGHTING FOR HEALTHCARE: QUANTUM DOT LIGHT-EMITTING DIODE-BASED PHOTOMEDICINE

QLEDs remarkably fits the light source profile currently required for widespread clinical adoption of phototherapies, in particular photodynamic therapy (PDT) and photobiomodulation (PBM). The efficacy and benefits of these phototherapies have already been clinically proven, however, important limitations of LED- and laser-based phototherapies are preventing their widespread adoption.[27] For instance, while laser systems are bulky and expensive, LED arrays have poor flexibility and inhomogeneous irradiance due to their point-source nature. While it is possible to add diffusers and optical fibers to obtain homogeneous flexible light sources out of lasers and LEDs, flexible QLEDs offer an ideal profile for a wearable photomedical light source considering multiple simultaneous benefits: simpler design and application; low cost; light, thin, and flexible form factors inherent to the device (no need for additional accessories); homogeneous large emission area; and capability for ambulatory or "at home" treatments. Furthermore, although flexible OLEDs have been proposed for several biomedical applications, including photomedicine,[103] OLEDs generally have low optical power density (OPD) and broad emission bandwidth at clinically relevant red wavelengths, and emission wavelength tunability needs additional structural design using the microcavity effect. In view of this, our group proposed the use of flexible QLEDs as alternative photo-

https://doi.org/10.1021/acsenergylett.1c02745
ACS Energy Lett. 2022, 7, 1001−1020

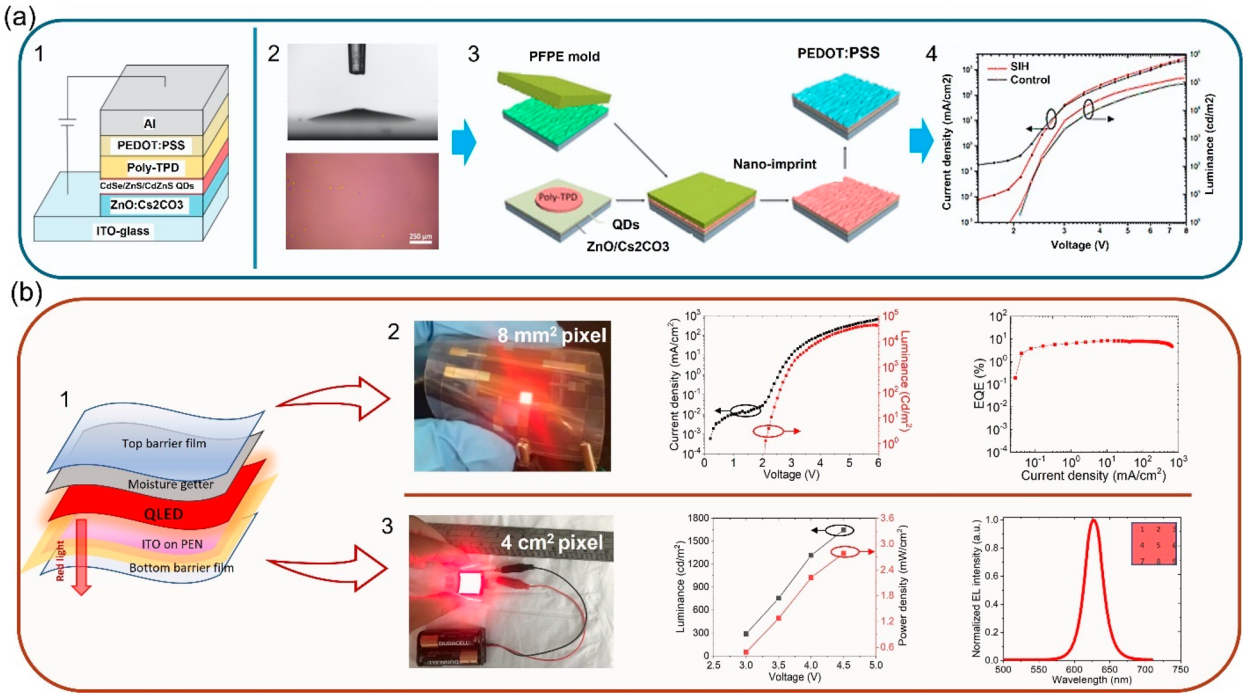

Figure 7. Progress in red-emitting QLEDs for photomedicine. (a-1) Cross-sectional scheme of QLEDs made by an all-solution process. (a-2) Contact angle image and optical microscopy image showing enhanced coverage of the poly-TPD surface after doping PEDOT:PSS with Triton X-100. Reproduced with permission from ref 104. Copyright 2018 RSC. (a-3) Scheme of the fabrication process of QLEDs with imprinted SIH nanostructures. (a-4) *J*−*L*−*V* curves of the SIH-QLED vs the planar QLED (control). Reproduced with permission from ref 105. Copyright 2019 ACS. (b-1) Structure of encapsulated flexible QLEDs. (b-2) Photograph (at 3.5 V in air), *J*−*L*−*V* curves, and EQE−*J* curve of flexible QLED with 8 mm² pixel. Reproduced with permission from ref 106. Copyright 2020 Wiley-VCH. (b-3) Photograph (at 3 V in air), *L*−OPD−*V* curves, and EL spectrum of flexible QLED with emitting area of 4 cm². Inset: Location of points measured on the emissive area (*L* @ 3 V). Reproduced with permission from ref 107. Copyright 2021 Proc IDW'21.

medical light sources, aiming to meet the need for a low-cost, ergonomic, homogeneous light source with sufficient power density (≥10 mW cm^{-2}) and narrow emission spectra (<30 nm) matching the absorption peaks of photosensitizers. Accordingly, our group has progressively developed QLEDs with clinically relevant red emission wavelengths. First, on-glass red-emitting QLEDs[94] with ultra-high brightness (1.65×10^5 cd m^{-2}) and a maximum EQE of ∼20% were achieved by both thermal evaporation and solution processes. Using accelerated testing in these devices, a half-lifetime (T50) of ∼93 h was estimated for an initial OPD of 10 mW cm^{-2}, which should guarantee sufficient dosage for PDT or PBM treatment sections, as subsequently demonstrated with in vitro testing. T50 is the time when the luminance has dropped to 50% of its initial value. Consecutively, QLEDs made by an all-solution process were reported; the devices had the structure shown in Figure 7a-1 and were achieved by doping the hole injection layer (PEDOT:PSS) with Triton X-100, as shown in Figure 7a-2.[104] Later, the performance of these QLEDs was improved (brightness up to 1.46×10^5 cd m^{-2}) by imprinting of speckle image holography (SIH) nanostructures on the surface of the hole transport layer (poly-TPD) surface;[105] a scheme of this method and the *J*−*L*−*V* curves are shown in Figure 7a-3 and a-4, respectively.

Subsequently, we focused on flexible QLEDs as they are in obligatory demand for wearable light source devices. Our best-performing flexible red-emitting QLEDs to date[106] were achieved by using flexible conductive substrates of indium tin oxide on polyethylene naphthalate (ITO-PEN) with a sheet resistance of 6−8 Ω/sq. The encapsulation of each device was performed as depicted in Figure 7b-1, and the composition of the barrier films was SiN−organic coating−SiN.[108] These flexible QLEDs with pixels of 8 mm^2 exhibited a record brightness of 4.22×10^4 cd m^{-2} at 5.8 V, peak EQE of 8.3%, and low efficiency roll-off over the measured range. Remarkably, the maximum corresponding OPD of ∼71 mW cm^{-2} largely surpassed the OPD required for low-irradiance PDT and PBM treatments (∼2−10 mW cm^{-2}). A picture of the flexible QLED with 8 mm^2 pixels, the corresponding *J*−*L*−*V* curves, and the EQE−*J* curve are presented in Figure 7b-2. It is worth noting that the structure and fabrication process of these preliminary flexible devices are similar to those of the on-glass QLEDs with maximum EQE of ∼20% mentioned above. Therefore, optimization of the thermal/barrier property and the CTLs of the flexible devices is expected to increase the EQE up to the theoretical limit (∼20%). In addition, this efficiency could be further increased by light outcoupling, as previously demonstrated for red-emitting flexible QLEDs with a record EQE of ∼25%.[109,110] Because of the need for large-area QLEDs for the photomedical treatment of large lesions, flexible ITO-PEN QLEDs with emitting area of 4 cm^2 were also achieved by the same fabrication process and inverted structure.[107] One picture of the QLED, the *L*−*V* curve and the corresponding OPD−*V* curve, and the EL spectrum are shown in Figure 7b-3. This large-area QLED weighed only 1.4 g and had red emission centered at 627 nm with fwhm ≈ 29 nm. In order to evaluate the homogeneity of the illumination area, the luminance (*L*) was measured at nine different positions of the emitting area (inset of the EL spectrum), and a relatively low standard deviation of 17% was obtained. Given the higher

https://doi.org/10.1021/acsenergylett.1c02745
ACS Energy Lett. 2022, 7, 1001−1020

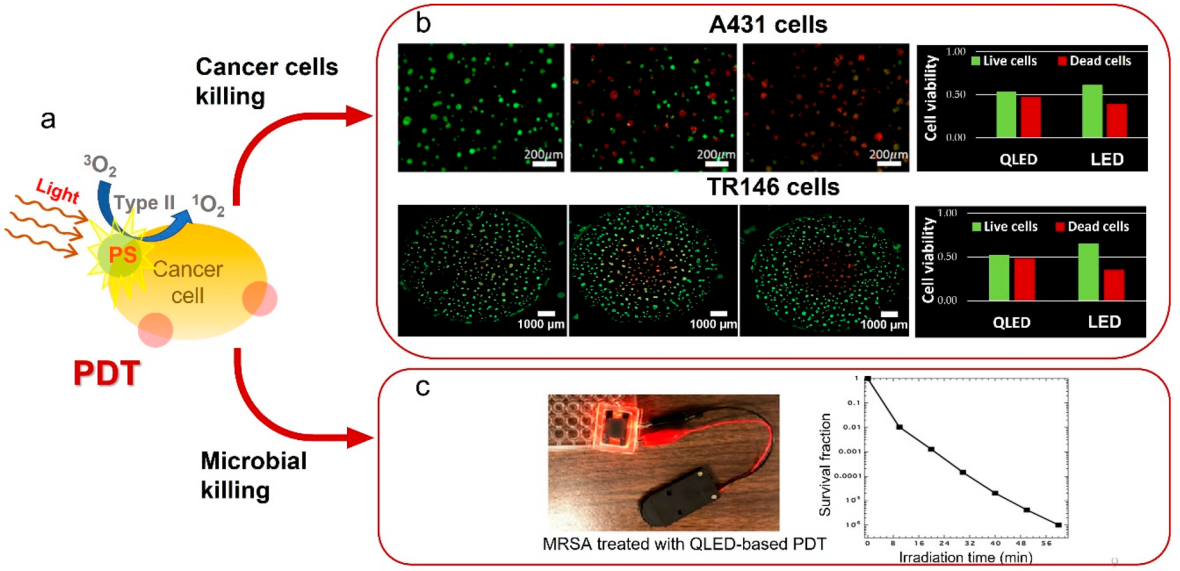

Figure 8. QLED-based PDT in vitro testing. (a) Illustration of the mechanism for PDT. $^3O_2$ is ground-state oxygen, and $^1O_2$ is singlet oxygen. (b) Fluorescent culture images 24 h post-PDT treatment and cell viability bar charts corresponding to A431[25] and TR146 cells.[107] The green and red dots correspond to live and dead cells, respectively. Cell cultures with QLED-based PDT (right), LED-based PDT (center), and without light treatment (left). (c) Survival fraction evolution of MRSA under QLED-based PDT.[26] Reproduced with permission from refs 25 and 26. Copyright 2017 and 2018 Wiley-VCH. Reproduced with permission from ref 107. Copyright 2021 Proc IDW'21.

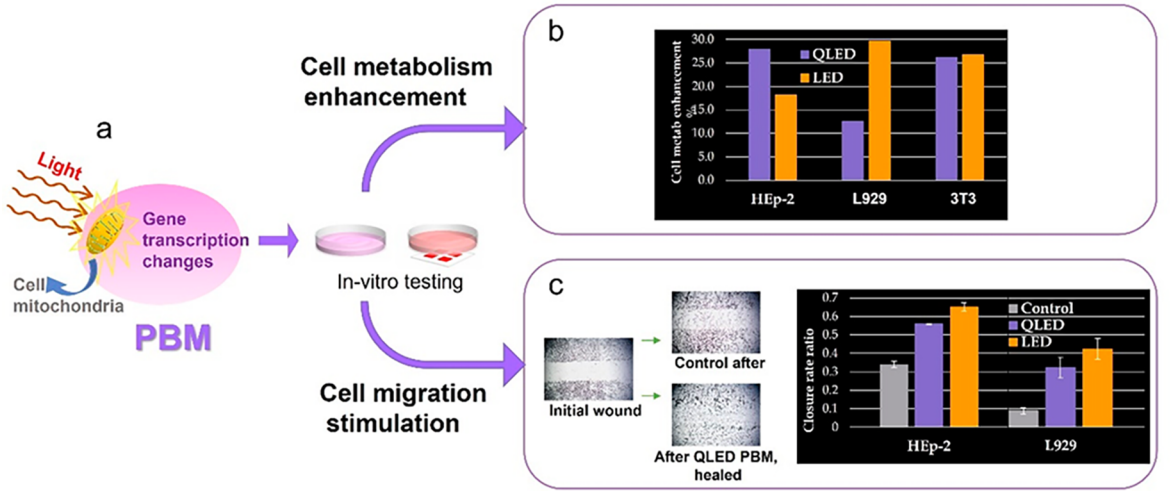

Figure 9. QLED-based PBM in vitro testing. (a) Basic scheme for the mechanism of action of PBM. (b) Cell metabolism enhancement of cells lines HEp-2, L929, and 3T3 after irradiation with either QLED or LED and with respect to control cultures. (c) Cell migration test based on a "2D scratch model". Closure rate ratio of cell lines HEp-2 and L929, 24 h after irradiation with QLED or LED and without irradiation.

current density driven through smaller pixels, the 8 mm^2 devices showed an exponential increase of the $L-V$ curve as compared with an almost linear increase in the case of the 4 cm^2 devices.

IN VITRO PHOTOBIOMODULATION AND PHOTODYNAMIC THERAPY FEASIBILITY DEMONSTRATION

PDT is effective for the treatment of diseases characterized by the presence of undesirable tissues and cells, such as cancer.[111] In addition, antimicrobial PDT is an alternative approach to inhibit the proliferation of pathogens.[112] In general, the mechanism of action for PDT needs the combination of light (the normal therapeutic window is 600−700 nm), a photosensitizer (i.e., a drug), and O_2 to produce reactive oxygen species (illustrated in Figure 8a). Consequently, these species kill and destroy the unwanted cells and tissues being targeted. Meanwhile, PBM therapy is known for the induction of beneficial clinical effects such as reduction of pain and inflammation, stimulation of wound healing, and hair regrowth.[113−116] The basic mechanism of PBM consists of exposure to red or near-infrared light, at specific irradiances and low doses, and subsequent absorption by endogenous cytochrome c oxidase, leading to a cascade of effects[117] (illustrated in Figure 9a). We proved the capability of QLEDs as photomedical light sources by PDT and PBM in vitro

https://doi.org/10.1021/acsenergylett.1c02745
ACS Energy Lett. 2022, 7, 1001−1020

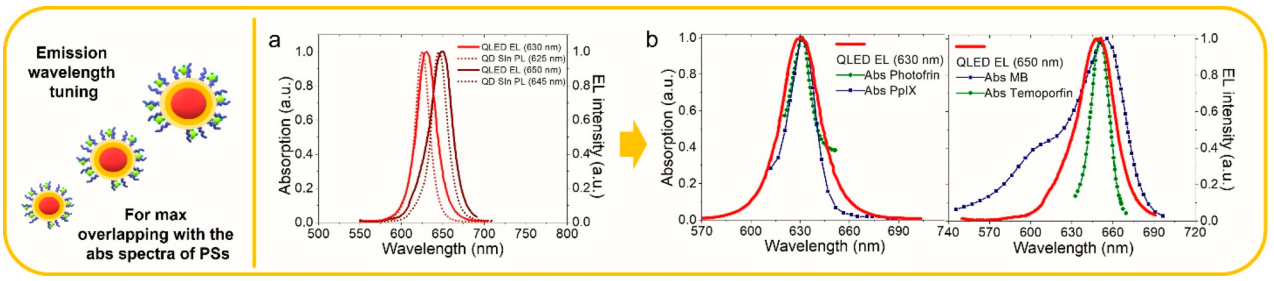

Figure 10. Controlled spectra overlapping for targeted phototherapy. (a) PL spectra of QDs in solution and EL spectra of the respective QLEDs. (b) Overlapping of the EL spectra of the QLEDs and absorption spectra of the corresponding photosensitizers: 630 nm QLED with Photofrin and PpIX, and 650 nm QLED with Temoporfin and MB.

testing and parallel comparison with the efficacy of commercial LEDs.

For the PDT in vitro tests, the cancer cells A431[25] and TR146[107] were treated using the photosensitizer Protoporphyrin IX (PpIX). While the A431 human cell line belongs to an epidermoid carcinoma in the skin, TR146 is a human squamous cell carcinoma whose primary tumor originated in the buccal mucosa. The fluorescent culture images taken 24 h post-treatment, on the left, and the corresponding cell viability bar charts, on the right, are shown for each cell culture in Figure 8b. Remarkably, the residual cell viabilities indicated higher efficacy in photo-destruction of cancer cells by QLED-based PDT as compared to LED-based PDT for both cell cultures. In addition to these PDT tests, an evaluation of the QLEDs efficacy in antimicrobial PDT was conducted.[26] Methicillin-resistant *Staphylococcus aureus* (MRSA) was treated with QLED-based PDT, which resulted in a significant survival fraction drop of less than 10^{-6} after 1 h treatment, as can be observed in Figure 8c. This result simultaneously demonstrated the high efficacy and simplicity of QLED-based antimicrobial PDT for infection treatment and promises inactivation of pathogens without the risk of inducing resistance.

In the first PBM in vitro study,[25,118] the QLED-based PBM treatment enhanced the cell metabolism of the HEp-2, L929, and 3T3 cell lines by 27.9, 12.5, and 26.2% over non-photoirradiated cultures, as shown in the bar chart of Figure 9b. Subsequently, another in vitro study to evaluate the effect of QLED-based PBM in wound healing was conducted using a "2D scratch model".[119] The best closure rate ratios at 24 h for the treatment of HEp-2 and L929 cell lines were increased 64% and 263% with respect to the control (see Figure 9c). Although the results were comparable, the mildly higher values observed for the commercial LEDs in both PBM experiments can be attributed to the longer emission wavelength of LEDs, given that longer red wavelengths are known to be more effective for PBM treatment. This suggested that further optimization can be achieved with QLEDs emitting at longer wavelengths.

TARGETED PHOTOTHERAPY DEMONSTRATION

In addition to the abovementioned in vitro photomedical studies, controlled spectra overlapping for targeted phototherapy was demonstrated by tuning the peak emission wavelength of the QDs.[107] First, QDs with high PLQY, narrow emission spectra (fwhm < 30 nm), and emission peaks at 625 and 646 nm were obtained by tuning the QDs' size during synthesis. Considering the Stark effect occurring in closely packed QD solid films under an external electric field, the ∼4−5 nm red-shift previously observed between the emission spectra peaks of QLEDs and the respective QD solutions was used for tuning the EL peak of the QLEDs (see Figure 10a). Subsequently, QLEDs with EL peak at 630 and 650 nm were obtained out of the synthesized QDs. These wavelengths were selected to match the absorption of four specific photosensitizers, the overlapping spectra is shown in Figure 10b.

QLEDs with EL peak at 630 nm match well with absorption peaks of Photofrin and PpIX (fourth Q-band), while QLEDs with EL peak at 650 nm can be used for excitation of Temoporfin and Methylene Blue (MB). Briefly, Photofrin is used for PDT treatments of cancer, endogenous PpIX for PDT treatment of actinic keratosis, Temoporfin for PDT treatment of head and neck squamous cell carcinoma, and MB for antibacterial and antiviral PDT. In addition to meeting these PDT needs, the 650 nm light has been demonstrated to stimulate cytochrome C oxidase for PBM treatment.

PERSPECTIVE ON QUANTUM DOTS-BASED ELECTROLUMINESCENCE FOR HEALTHCARE

While QDs-based EL has been mainly researched for display applications, we believe that photomedicine will be one initial market where QLEDs can have commercial success with significant social benefits. The high potential of QLEDs to escalate the adoption of photomedicine promises wide coverage of multiple healthcare markets such as cancer treatment, periodontal disease, dermatology (especially cosmetic dermatology), and chronic wound and ulcer care. Initially, a single market targeting the treatments and settings where QLEDs are currently most needed is necessary. We propose PDT treatment of oral cancer and PBM treatment for diabetic wound healing as target treatments for initial photomedical applications of flexible QLEDs. Accordingly, the high incidence of oral cancer in low-resource populations (e.g., in India), the high cost and negative side effects of current treatments, and the limitations of mainstream light sources for wide adoption of PDT, are demanding an alternative cost-effective light source. In addition, the unsatisfactory results of existing multidisciplinary treatments for impaired wound healing, also merit the introduction of QLEDs for targeted PBM. The introduction of QLEDs in the photomedicine market can be a challenging pathway due to the multidisciplinary nature of the application, however, synergetic progress on the device development, medical treatments with photomedicine experts, and regulatory clearance process, will be the key factors to guarantee the final commercialization of QLEDs as photomedical light sources.

https://doi.org/10.1021/acsenergylett.1c02745
ACS Energy Lett. 2022, 7, 1001−1020

To date, our QLEDs fulfilled several needs for photomedical application, and the QLED-based in vitro studies also showed satisfactory results comparable to those of commercial LED-based studies. However, to put the progress status in perspective, we briefly discuss key technical developments required to advance the application of flexible QLEDs in photomedicine.

Thermal management, effective encapsulation, and integration into wearable devices are key technical developments required to advance the application of flexible QLEDs in photomedicine.

Safety is a critical requirement for the direct application of QLED devices on patients, therefore QLED overheating during operation needs to be prevented via thermal management. QLEDs are inherent area emitters that can dissipate heat over the whole device area and thus are normally considered low-heat light sources; however, flexible QLEDs on plastic substrates have poor heat dissipation due to the low thermal diffusivity of polymers (e.g., PET and PEN). Systematic steps should be followed to increase the EQE and consequently reduce the Joule-heat generation at high brightness, once this optimization has been performed, thermal management of the QLEDs through heat dissipation is reasonable. This is relevant for the integration of flexible QLEDs in bandage-type devices and their application for the treatment of the skin. Overall, direct contact of the QLED emitting surface with the skin maybe undesirable, in particular for the treatment of conditions such as diabetic wounds and superficial infections. Therefore, a small space between the skin and the emitting surface maybe required, along with the use of a wound dressing in between. The closer the emitting area, the better the irradiation at the skin surface; therefore, the emitting surface of the QLED should have a safe temperature during phototherapy. Here, we simulated the heat transfer of 8 mm^2 pixel flexible devices with the characteristic performance shown in Figure 7b-2 and the structure PEN barrier–ITO/QLED/PEN barrier, where the bottom surface of the PEN barrier–ITO substrate corresponds to the emitting surface. Also, a small cavity between the emitting surface of the QLED and the skin surface was considered for the simulation. In such a cavity, the air temperature was approximated as the average temperature of the human skin, ~33 °C, while the room temperature of the air was 25 °C (in contact with the top of the QLED). Heat transfer simulation was performed using cylindrical coordinates (circle pixel) and the finite element method (FEM) in COMSOL. This first simulation showed that the temperature

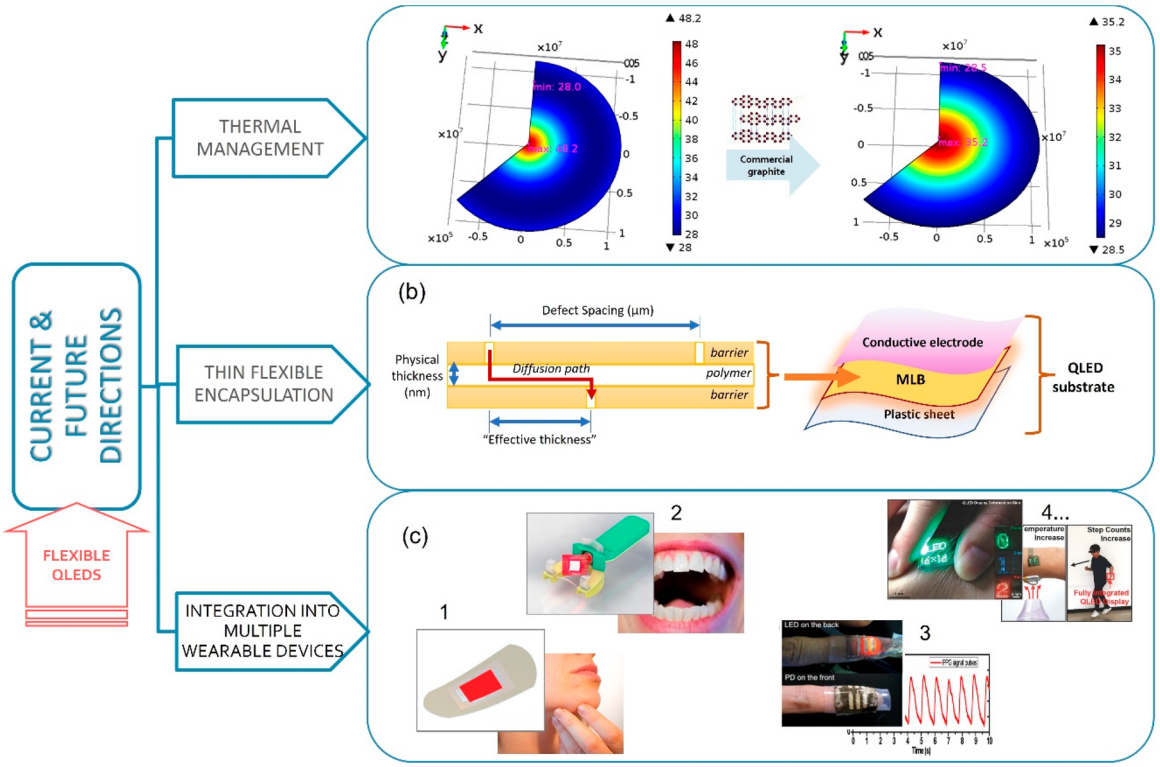

Figure 11. Current and future directions for the development of flexible QLEDs as wearable devices. (a) Steady-state thermal profiles simulated with COMSOL for a PEN barrier–ITO/QLED/PEN barrier device (left) and a PEN barrier–ITO/QLED/graphite sheet/PEN barrier device (right) with increased heat dissipation. The view corresponds to the emitting surface of the QLED devices. (b) Cross-sectional scheme of an MLB (left) and ideal integration of the MLB in the flexible conductive substrate (right). (c-1) Conceptual design of a bandage-type QLED device for phototherapy of skin diseases and conditions. (c-2) Conceptual design of a mouthguard-type QLED device for phototherapy of the oral cavity. (c-3) Epidermal sensor with wavy red QLEDs and QD-PD wrapped around a forefinger for recording of photoplethysmographic signals. Reproduced with permission from ref 120. Copyright 2017 ACS. (c-4) Ultra-thin QLED display on deformed skin. The integrated wearable system visualized the real-time ambient temperature and the wearer's step count. Reproduced with permission from ref 121. Copyright 2018 Wiley-VCH.

https://doi.org/10.1021/acsenergylett.1c02745
ACS Energy Lett. 2022, 7, 1001–1020

on the top and bottom (emitting surface) surfaces can rise above 40 °C at the steady state when the devices are operated around the maximum EQE (thermal profile in Figure 11a, left). A QLED with a surface temperature ≥40 °C could cause discomfort and even superficial burns on the skin. It is worth noting that the ∼zero temperature gradient across the thickness and the high gradient in the planar direction of the device are in accordance with the high aspect ratio of this kind of device (width/thickness ≫ 1). Subsequently, simulations of the heat transfer using heat sink materials on top of the QLED (PEN barrier−ITO/QLED/heat sink sheet/PEN barrier) were also performed. Importantly, this management demonstrated that commercial flexible graphite sheets with anisotropic thermal conductivity (κ) can effectively assist in heat dissipation by significantly reducing the QLED surface temperature, as shown in the thermal profiles from Figure 11a (from 48 to 35 °C). The characteristic conductive heat transport of graphite sheets is efficient for planar devices with a very high aspect ratio, given that the microscale thickness of the QLED device compensates the low κ (3.4 W m^{-1} K^{-1}) in the vertical direction, while the high κ (1850 W m^{-1} K^{-1}) in the planar direction compensates the macroscale sides of the device. Lamination of graphite sheets makes thermal management simpler, and further testing of these results should guarantee a QLED surface temperature close to the average temperature of the human skin over a wide operating range.

In addition, an effective barrier against moisture and oxygen to avoid quick degradation of the flexible QLEDs is needed. In this regard, the thin-film encapsulation consisting in a hybrid multilayer barrier (MLB) is a highly reliable technique. In an MLB "1 inorganic layer + 1 organic layer" represents one dyad, while the inorganic layers act as thin barriers, the organic layers mitigate the defect growth and increase the diffusion path of water and oxygen, as illustrated in Figure 11b (left). Thin-film encapsulation is typically formed by chemical vapor deposition or atomic layer deposition of nanoscale inorganic layers alternated with solution-processing of polymer-based organic layers. When this process is conducted immediately after the device fabrication, the barrier property of the device can reach a very low water vapor transmission rate (∼10^{-6} g m^{-2} d^{-1}). Alternatively, the dyads can first be deposited on plastic substrates and then be used as bottom substrates and top barriers of flexible devices, as demonstrated before for OLEDs.[122] An MLB integrated between the conductive electrode and the plastic substrate, as illustrated in Figure 11b (right), should significantly improve the shelf life of the devices as compared to the bottom lamination method described in a previous section (Figure 7b-1). Additionally, the insertion of more dyads with the state-of-the-art barrier materials (e.g., ZnO, MgO, Al_2O_3) into the MLB could improve the barrier property of the flexible devices in comparison to the MLB described before (1.5 dyads). It is worth noting that flexible barrier lamination is compatible with high-volume manufacturing through roll-to-roll processing, and due to the similar nature of OLEDs and QLEDs, this mature encapsulation strategy can be adopted with QLEDs. However, the low throughput of thin-film encapsulation imposed by the deposition chamber size makes necessary novel approaches for the continuous production of large-area devices.

Ultimately, the design of QLED-based medical devices may vary significantly between different photomedical applications. However, thin, lightweight, flexible QLEDs offer unique advantages over commercial light sources, since they can be used as a universal platform for integration to different devices and treatment of locations with different spatial characteristics. Naturally, treatment of easy-to-access locations are preferred for early application of QLEDs. We suggest the skin and the oral cavity as initial targeted treatments and the following conceptual designs of wearable devices for ambulatory or "at home" treatment. A bendable bandage-type device as sketched in Figure 11c-1 will be ideal for treatment of skin conditions. Such a bandage should be adhesive on the edges and contain both the flexible QLED and the power source. Meanwhile, a mouthguard-type device will be ideal for treatment of the oral cavity, an early conceptual design is shown in Figure 11c-2. The flexible QLEDs supported in this oral plastic device are expected to irradiate different soft tissues, mainly the tongue, hard and soft palate, and the buccal mucosa. The integration of QLED light sources to make disposable medical sensors for pulse oximetry is another potential application being explored. Kim et al.[120] reported a fully stretchable QD-based sensor integrated by a QLED and a QD photodetector for monitoring of blood waves via recording of photoplethysmographic signals (see Figure 11c-3). The great potential of QLEDs also promises the integration of QLED-based displays as information input/output ports in all kinds of wearable devices to monitor different functions.[123] For instance, Kim et al.[121] reported a fully integrated QLED display with a touch user interface that directly showed sensor data (shown in Figure 11c-4).

Finally, the integration of QLEDs into wearable optoelectronics with the potential to promote new paradigms, such as "at home" health monitoring and therapy, is attracting growing interest. We believe that our research in QLED-based photomedicine along with the parallel research conducted by other groups will drive the application of flexible QLEDs in wearable optoelectronic devices. It is also worth noting that the low-cost solution processing, narrow emission fwhm, high OPD, and simple emission wavelength tunability of QLEDs offer important advantages over other flexible light sources such as OLEDs, making QLEDs highly competitive for future photomedical and biomedical applications (i.e., sensing, optogenetics, lab/organ-on-a-chip, etc.)[120,124−126] in the healthcare spectrum. Preliminary research in QLED-based photomedicine has been conducted primarily through in vitro studies using rigid on-glass QLEDs. Therefore, advancement of the photomedical studies to in vivo testing with flexible QLEDs will be necessary to de-risk the technology for subsequent human clinical trials and the U.S. Food & Drug Administration (FDA) clearance or approval.

Overall, it has been demonstrated that both QDs and PNCs exhibit multiple benefits when applied as light converters in display devices, or even as self-emissive materials in emerging applications such as photomedicine requiring ergonomic form factors, emission tunability, low-cost processing, and other special features. On one hand, the integration of these outstanding luminescent nanomaterials through the CEF and CC technologies have the potential to enhance the performance of the current display technologies in terms of color volume and power consumption. Meanwhile, the simpler but promising development of wearable QLEDs have the potential to enable wider adoption of PDT and PBM treatments by offering light, thin, and flexible form factors, cost-effective fabrication, narrow emission bandwidth, and high OPD at clinically relevant red wavelengths. Remarkably, the current record EQE of red-emitting flexible QLEDs (∼25%) makes

https://doi.org/10.1021/acsenergylett.1c02745
ACS Energy Lett. 2022, 7, 1001−1020

them competitive with state-of-the-art inorganic LEDs and OLEDs in terms of efficiency, and there is still room for efficiency improvement by light outcoupling. As discussed here, encapsulation, thermal management, and large-scale integration are some of the key technical developments to push forward these applications. We expect that with the roadmap paved by the primitive QDs (e.g., CdSe QDs) and the increased worldwide efforts, a faster development and commercialization of stable and heavy-metal-free QDs and PNCs will be possible through display and healthcare technologies.

AUTHOR INFORMATION

Corresponding Authors

Yajie Dong − *NanoScience Technology Center, University of Central Florida, Orlando, Florida 32826, United States; College of Optics and Photonics and Department of Materials Science and Engineering, University of Central Florida, Orlando, Florida 32816, United States; QLEDcures LLC, Orlando, Florida 32826, United States;* orcid.org/0000-0001-5319-2462; Email: yajie.dong@ucf.edu

Shin-Tson Wu − *College of Optics and Photonics, University of Central Florida, Orlando, Florida 32816, United States;* orcid.org/0000-0002-0943-0440; Email: swu@creol.ucf.edu

Authors

Manuel A. Triana − *NanoScience Technology Center, University of Central Florida, Orlando, Florida 32826, United States; College of Optics and Photonics, University of Central Florida, Orlando, Florida 32816, United States*

En-Lin Hsiang − *College of Optics and Photonics, University of Central Florida, Orlando, Florida 32816, United States*

Caicai Zhang − *NanoScience Technology Center, University of Central Florida, Orlando, Florida 32826, United States; Department of Materials Science and Engineering, University of Central Florida, Orlando, Florida 32816, United States*

Complete contact information is available at: https://pubs.acs.org/10.1021/acsenergylett.1c02745

Notes

The authors declare the following competing financial interest(s): Y.D. is a co-founder and chief scientific officer of QLEDCures, LLC, a start-up company focusing on QLED development for photomedical applications.

Biographies

Manuel A. Triana is a postdoctoral fellow at the NanoScience Technology Center and the College of Optics and Photonics of the University of Central Florida. He received his M.E. and Ph.D. degrees in chemical engineering from Universidad del Valle, Colombia. His current research focuses on quantum dot materials and their light-emitting devices for display, lighting, and photomedicine.

En-Lin Hsiang is working toward the Ph.D. degree at the College of Optics and Photonics, University of Central Florida. His current research focuses on display technologies including LCDs, OLED, μLED, and mini-LED displays and projection display systems for AR/VR headsets.

Caicai Zhang received her M.S. degree from the University of Florida in 2016 and Ph.D. degree from the University of Central Florida in 2021, both in materials science and engineering. She is currently working at Corning, Inc. as a Display Innovation Specialist.

Yajie Dong is an associate professor at the Nanoscience Technology Center and Department of Materials Science & Engineering of the University of Central Florida, with a joint appointment in the College of Optics and Photonics. He received his B.S. and M.S. degrees from Tsinghua University, China, and his Ph.D. degree from Harvard University. http://www.nanoscience.ucf.edu/dong/people.php

Shin-Tson Wu is a Pegasus professor in the College of Optics and Photonics, University of Central Florida. He is the recipient of the 2022 SPIE Maria Goeppert Mayer award, 2014 OSA Esther Hoffman Beller medal, 2011 SID Slottow-Owaki prize, 2010 OSA Joseph Fraunhofer award, 2008 SPIE G. G. Stokes award, and 2008 SID Jan Rajchman prize. https://lcd.creol.ucf.edu/

ACKNOWLEDGMENTS

The authors would like to thank our collaborators (Dr. Andre J. Gesquiere of University of Central Florida (UCF), Drs. Ziqian He and Hao Chen of Apple, Dr. Raymond Lanzafame of QLEDCures, Dr. Jonathan Celli of University of Massachusetts Boston, Dr. Michael Hamblin of University of Johannesburg in South Africa, and Dr. Shun-Wei Liu of Ming Chi University of Technology in Taiwan) and Dr. Tayyaba Hasan of Harvard Medical School and Wellman Center for Photomedicine for helpful discussions and/or their respective contributions to data reported in our previous publications summarized in this Perspective. Y.D. acknowledges UCF for a NSTC seed grant (No. 63014223), the American Society for Laser Medicine and Surgery, Inc. (ASLMS), and the Community Foundation of North Central Wisconsin for A. Ward Ford Memorial Research Grant support, and thanks QLEDCures and National Science Foundation (NSF) for an STTR award (1843101). S.-T.W. is indebted to a.u.Vista, Inc. and Nichia Corp. for financial support.

REFERENCES

(1) Bourzac, K. Quantum dots go on display. *Nature* **2013**, *493* (7432), 283−283.

(2) Steckel, J. S.; Ho, J.; Hamilton, C.; Xi, J.; Breen, C.; Liu, W.; Allen, P.; Coe-Sullivan, S. Quantum dots: The ultimate down-conversion material for LCD displays. *J. Soc. Inf. Dispersion* **2015**, *23* (7), 294−305.

(3) Erdem, T.; Demir, H. V. Colloidal nanocrystals for quality lighting and displays: milestones and recent developments. *Nanophotonics* **2016**, *5* (1), 74−95.

(4) Luo, Z.; Yurek, J. *Quantum dots: the technology platform for all future displays*; SPIE: 2019; Vol. *10940*.

(5) Shu, Y.; Lin, X.; Qin, H.; Hu, Z.; Jin, Y.; Peng, X. Quantum Dots for Display Applications. *Angew. Chem., Int. Ed.* **2020**, *59* (50), 22312−22323.

(6) Kojima, A.; Ikegami, M.; Teshima, K.; Miyasaka, T. Highly Luminescent Lead Bromide Perovskite Nanoparticles Synthesized with Porous Alumina Media. *Chem. Lett.* **2012**, *41* (4), 397−399.

(7) Schmidt, L. C.; Pertegás, A.; González-Carrero, S.; Malinkiewicz, O.; Agouram, S.; Mínguez Espallargas, G.; Bolink, H. J.; Galian, R. E.; Pérez-Prieto, J. Nontemplate Synthesis of CH3NH3PbBr3 Perovskite Nanoparticles. *J. Am. Chem. Soc.* **2014**, *136* (3), 850−853.

(8) Protesescu, L.; Yakunin, S.; Bodnarchuk, M. I.; Krieg, F.; Caputo, R.; Hendon, C. H.; Yang, R. X.; Walsh, A.; Kovalenko, M. V. Nanocrystals of Cesium Lead Halide Perovskites (CsPbX3, X = Cl, Br, and I): Novel Optoelectronic Materials Showing Bright Emission with Wide Color Gamut. *Nano Lett.* **2015**, *15* (6), 3692−3696.

(9) Zhang, F.; Zhong, H.; Chen, C.; Wu, X.-g.; Hu, X.; Huang, H.; Han, J.; Zou, B.; Dong, Y. Brightly Luminescent and Color-Tunable Colloidal CH3NH3PbX3 (X = Br, I, Cl) Quantum Dots: Potential Alternatives for Display Technology. *ACS Nano* **2015**, *9* (4), 4533−4542.

(10) Kim, T.-H.; Cho, K.-S.; Lee, E. K.; Lee, S. J.; Chae, J.; Kim, J. W.; Kim, D. H.; Kwon, J.-Y.; Amaratunga, G.; Lee, S. Y.; Choi, B. L.; Kuk, Y.; Kim, J. M.; Kim, K. Full-colour quantum dot displays fabricated by transfer printing. *Nat. Photonics* **2011**, *5* (3), 176−182.
(11) Wang, T.; Zhang, Y.; Gao, Y.; Zhang, Z.; Chen, Z.; Li, D.; Mei, W.; Li, Y.; Zhou, L.; Pei, C.; Yu, J.; Shi, H.; Liao, J.; Li, X.; Xu, X. 63−4: Development of Ink-jet Printing Process for 55-in. UHD AMQLED Display. *SID Int. Symp. Dig Tec* **2021**, *52* (1), 930−932.
(12) Won, Y.-H.; Cho, O.; Kim, T.; Chung, D.-Y.; Kim, T.; Chung, H.; Jang, H.; Lee, J.; Kim, D.; Jang, E. Highly efficient and stable InP/ZnSe/ZnS quantum dot light-emitting diodes. *Nature* **2019**, *575* (7784), 634−638.
(13) Jang, E.; Kim, Y.; Won, Y.-H.; Jang, H.; Choi, S.-M. Environmentally Friendly InP-Based Quantum Dots for Efficient Wide Color Gamut Displays. *ACS Energy Lett.* **2020**, *5* (4), 1316−1327.
(14) Kim, T.; Kim, K.-H.; Kim, S.; Choi, S.-M.; Jang, H.; Seo, H.-K.; Lee, H.; Chung, D.-Y.; Jang, E. Efficient and stable blue quantum dot light-emitting diode. *Nature* **2020**, *586* (7829), 385−389.
(15) Wu, Z.; Liu, P.; Zhang, W.; Wang, K.; Sun, X. W. Development of InP Quantum Dot-Based Light-Emitting Diodes. *ACS Energy Lett.* **2020**, *5* (4), 1095−1106.
(16) Han, M. G.; Lee, Y.; Kwon, H.-i.; Lee, H.; Kim, T.; Won, Y.-H.; Jang, E. InP-Based Quantum Dot Light-Emitting Diode with a Blended Emissive Layer. *ACS Energy Lett.* **2021**, *6* (4), 1577−1585.
(17) Choi, M. K.; Yang, J.; Kang, K.; Kim, D. C.; Choi, C.; Park, C.; Kim, S. J.; Chae, S. I.; Kim, T.-H.; Kim, J. H. J. N. c.; et al. Wearable red−green−blue quantum dot light-emitting diode array using high-resolution intaglio transfer printing. *Nat. Commun.* **2015**, *6* (1), 7149.
(18) Kim, B. H.; Onses, M. S.; Lim, J. B.; Nam, S.; Oh, N.; Kim, H.; Yu, K. J.; Lee, J. W.; Kim, J.-H.; Kang, S.-K.; Lee, C. H.; Lee, J.; Shin, J. H.; Kim, N. H.; Leal, C.; Shim, M.; Rogers, J. A. High-Resolution Patterns of Quantum Dots Formed by Electrohydrodynamic Jet Printing for Light-Emitting Diodes. *Nano Lett.* **2015**, *15* (2), 969−973.
(19) Wang, Y.; Fedin, I.; Zhang, H.; Talapin, D. V. Direct optical lithography of functional inorganic nanomaterials. *Science* **2017**, *357* (6349), 385−388.
(20) Shirasaki, Y.; Supran, G. J.; Bawendi, M. G.; Bulović, V. Emergence of colloidal quantum-dot light-emitting technologies. *Nat. Photonics* **2013**, *7* (1), 13−23.
(21) Yang, J.; Choi, M. K.; Yang, U. J.; Kim, S. Y.; Kim, Y. S.; Kim, J. H.; Kim, D.-H.; Hyeon, T. Toward Full-Color Electroluminescent Quantum Dot Displays. *Nano Lett.* **2021**, *21* (1), 26−33.
(22) MacLaughlin, C. M. Opportunities and Challenges in Perovskite-Based Display Technologies: A Conversation with Andrey Rogach and Haibo Zeng. *ACS Energy Letters* **2019**, *4* (4), 977−979.
(23) Wei, Z.; Xing, J. The Rise of Perovskite Light-Emitting Diodes. *J. Phys. Chem. Lett.* **2019**, *10* (11), 3035−3042.
(24) Li, Y.-F.; Feng, J.; Sun, H.-B., Perovskite Quantum Dots Based Light-Emitting Diodes. In *Perovskite Quantum Dots*; Zhou, Y., Wang, Y.,, Eds.; Springer: Singapore, 2020; Vol. *303*.
(25) Chen, H.; He, J.; Lanzafame, R.; Stadler, I.; Hamidi, H. E.; Liu, H.; Celli, J.; Hamblin, M. R.; Huang, Y.; Oakley, E.; Shafirstein, G.; Chung, H.-K.; Wu, S.-T.; Dong, Y. Quantum dot light emitting devices for photomedical applications. *J. Soc. Inf. Dispersion* **2017**, *25* (3), 177−184.
(26) Chen, H.; Yeh, T.-H.; He, J.; Zhang, C.; Abbel, R.; Hamblin, M. R.; Huang, Y.; Lanzafame, R. J.; Stadler, I.; Celli, J.; Liu, S.-W.; Wu, S.-T.; Dong, Y. Flexible quantum dot light-emitting devices for targeted photomedical applications. *J. Soc. Inf. Dispersion* **2018**, *26* (5), 296−303.
(27) Triana, M. A.; Restrepo, A. A.; Lanzafame, R. J.; Palomaki, P.; Dong, Y. Quantum dot light-emitting diodes as light sources in photomedicine: photodynamic therapy and photobiomodulation. *JPhys. Materials* **2020**, *3* (3), 032002.
(28) Chen, H.-W.; Zhu, R.-D.; He, J.; Duan, W.; Hu, W.; Lu, Y.-Q.; Li, M.-C.; Lee, S.-L.; Dong, Y.-J.; Wu, S.-T. Going beyond the limit of an LCD's color gamut. *Light: Science & Applications* **2017**, *6* (9), e17043−e17043.
(29) Yang, J. P.; Hsiang, E. L.; Chen, H. M. P. In *4-3: Wide Viewing Angle TN LCD Enhanced by Printed Quantum-Dots Film*; SID Int. Symp. Dig. Tech. Paper, Wiley Online Library: 2016; pp 21−24.
(30) Srivastava, A. K.; Zhang, W.; Schneider, J.; Halpert, J. E.; Rogach, A. L. Luminescent Down-Conversion Semiconductor Quantum Dots and Aligned Quantum Rods for Liquid Crystal Displays. *Adv. Sci.* **2019**, *6* (22), 1901345.
(31) Hu, Z.; Yin, Y.; Ali, M. U.; Peng, W.; Zhang, S.; Li, D.; Zou, T.; Li, Y.; Jiao, S.; Chen, S.-j.; Lee, C.-Y.; Meng, H.; Zhou, H. Inkjet printed uniform quantum dots as color conversion layers for full-color OLED displays. *Nanoscale* **2020**, *12* (3), 2103−2110.
(32) Yin, Y.; Hu, Z.; Ali, M. U.; Duan, M.; Gao, L.; Liu, M.; Peng, W.; Geng, J.; Pan, S.; Wu, Y.; et al. Full-color micro-LED display with CsPbBr3 perovskite and CdSe quantum dots as color conversion layers. *Adv. Mater. Technol.* **2020**, *5* (8), 2000251.
(33) Lee, J.-H.; Chen, C.-H.; Lee, P.-H.; Lin, H.-Y.; Leung, M.-k.; Chiu, T.-L.; Lin, C.-F. Blue organic light-emitting diodes: current status, challenges, and future outlook. *J. Mater. Chem. C* **2019**, *7* (20), 5874−5888.
(34) Chan, C.-Y.; Tanaka, M.; Lee, Y.-T.; Wong, Y.-W.; Nakanotani, H.; Hatakeyama, T.; Adachi, C. Stable pure-blue hyperfluorescence organic light-emitting diodes with high-efficiency and narrow emission. *Nat. Photon* **2021**, *15* (3), 203−207.
(35) Tan, G.; Lee, J.-H.; Lin, S.-C.; Zhu, R.; Choi, S.-H.; Wu, S.-T. Analysis and optimization on the angular color shift of RGB OLED displays. *Opt. Express* **2017**, *25* (26), 33629−33642.
(36) Kawanishi, H.; Onuma, H.; Maegawa, M.; Kurisu, T.; Ono, T.; Akase, S.; Yamaguchi, S.; Momotani, N.; Fujita, Y.; Kondo, Y.; et al. High-resolution and high-brightness full-colour "Silicon Display" for augmented and mixed reality. *J. Soc. Inf. Dispersion* **2021**, *29* (1), 57−67.
(37) Lee, E.; Tangirala, R.; Smith, A.; Carpenter, A.; Hotz, C.; Kim, H.; Yurek, J.; Miki, T.; Yoshihara, S.; Kizaki, T.; Ishizuka, A.; Kiyoto, I. 41−5: Invited Paper: Quantum Dot Conversion Layers Through Inkjet Printing. *SID Int. Symp. Dig Tec* **2018**, *49* (1), 525−527.
(38) Li, L.; Tang, G.; Shi, Z.; Ding, H.; Liu, C.; Cheng, D.; Zhang, Q.; Yin, L.; Yao, Z.; Duan, L.; Zhang, D.; Wang, C.; Feng, M.; Sun, Q.; Wang, Q.; Han, Y.; Wang, L.; Luo, Y.; Sheng, X. Transfer-printed, tandem microscale light-emitting diodes for full-color displays. *Proc. Natl. Acad. Sci. U.S.A.* **2021**, *118* (18), e2023436118.
(39) Shen, Y. C.; Mueller, G. O.; Watanabe, S.; Gardner, N. F.; Munkholm, A.; Krames, M. R. Auger recombination in InGaN measured by photoluminescence. *Appl. Phys. Lett.* **2007**, *91* (14), 141101.
(40) Mitchell, B.; Dierolf, V.; Gregorkiewicz, T.; Fujiwara, Y. Perspective: Toward efficient GaN-based red light emitting diodes using europium doping. *J. Appl. Phys.* **2018**, *123* (16), 160901.
(41) Iida, D.; Zhuang, Z.; Kirilenko, P.; Velazquez-Rizo, M.; Najmi, M. A.; Ohkawa, K. 633-nm InGaN-based red LEDs grown on thick underlying GaN layers with reduced in-plane residual stress. *Appl. Phys. Lett.* **2020**, *116* (16), 162101.
(42) Medintz, I. L.; Mattoussi, H. Quantum dot-based resonance energy transfer and its growing application in biology. *Phys. Chem. Chem. Phys.* **2009**, *11* (1), 17−45.
(43) Noh, M.; Kim, T.; Lee, H.; Kim, C.-K.; Joo, S.-W.; Lee, K. Fluorescence quenching caused by aggregation of water-soluble CdSe quantum dots. *Colloids Surf. A: Physicochem. Eng. Asp.* **2010**, *359* (1), 39−44.
(44) Coropceanu, I.; Bawendi, M. G. Core/Shell Quantum Dot Based Luminescent Solar Concentrators with Reduced Reabsorption and Enhanced Efficiency. *Nano Lett.* **2014**, *14* (7), 4097−4101.
(45) Meinardi, F.; Colombo, A.; Velizhanin, K. A.; Simonutti, R.; Lorenzon, M.; Beverina, L.; Viswanatha, R.; Klimov, V. I.; Brovelli, S. Large-area luminescent solar concentrators based on 'Stokes-shift-engineered' nanocrystals in a mass-polymerized PMMA matrix. *Nat. Photon* **2014**, *8* (5), 392−399.

https://doi.org/10.1021/acsenergylett.1c02745
ACS Energy Lett. 2022, 7, 1001−1020

(46) Chou, K. F.; Dennis, A. M. Förster Resonance Energy Transfer between Quantum Dot Donors and Quantum Dot Acceptors. *Sensors (Basel, Switzerland)* **2015**, *15* (6), 13288−325.
(47) Sadeghi, S.; Bahmani Jalali, H.; Melikov, R.; Ganesh Kumar, B.; Mohammadi Aria, M.; Ow-Yang, C. W.; Nizamoglu, S. Stokes-Shift-Engineered Indium Phosphide Quantum Dots for Efficient Luminescent Solar Concentrators. *ACS Appl. Mater. Interfaces* **2018**, *10* (15), 12975−12982.
(48) Sadeghi, S.; Ganesh Kumar, B.; Melikov, R.; Mohammadi Aria, M.; Bahmani Jalali, H.; Nizamoglu, S. Quantum dot white LEDs with high luminous efficiency. *Optica* **2018**, *5* (7), 793−802.
(49) Kim, H.; Shin, M.; Hong, H.; Song, B.; Kim, S.; Koo, W.; Yoon, J.; Yoon, S.; Kim, Y. Enhancement of Optical Efficiency in White OLED Display Using the Patterned Photoresist Film Dispersed With Quantum Dot Nanocrystals. *J. Dispersion Technol.* **2016**, *12* (6), 526−531.
(50) Jun, S.; Lee, J.; Jang, E. Highly Luminescent and Photostable Quantum Dot−Silica Monolith and Its Application to Light-Emitting Diodes. *ACS Nano* **2013**, *7* (2), 1472−1477.
(51) Smith, M. J.; Malak, S. T.; Jung, J.; Yoon, Y. J.; Lin, C. H.; Kim, S.; Lee, K. M.; Ma, R.; White, T. J.; Bunning, T. J.; Lin, Z.; Tsukruk, V. V. Robust, Uniform, and Highly Emissive Quantum Dot−Polymer Films and Patterns Using Thiol−Ene Chemistry. *ACS Appl. Mater. Interfaces* **2017**, *9* (20), 17435−17448.
(52) Moon, H.; Lee, C.; Lee, W.; Kim, J.; Chae, H. Stability of Quantum Dots, Quantum Dot Films, and Quantum Dot Light-Emitting Diodes for Display Applications. *Adv. Mater.* **2019**, *31* (34), 1804294.
(53) Kim, Y. H.; Koh, S.; Lee, H.; Kang, S.-M.; Lee, D. C.; Bae, B.-S. Photo-Patternable Quantum Dots/Siloxane Composite with Long-Term Stability for Quantum Dot Color Filters. *ACS Appl. Mater. Interfaces* **2020**, *12* (3), 3961−3968.
(54) Lee, S.; Lee, C. High-density quantum dots composites and its photolithographic patterning applications. *Polym. Adv. Technol.* **2019**, *30* (3), 749−754.
(55) Lin, H.-Y.; Sher, C.-W.; Hsieh, D.-H.; Chen, X.-Y.; Chen, H.-M. P.; Chen, T.-M.; Lau, K.-M.; Chen, C.-H.; Lin, C.-C.; Kuo, H.-C. Optical cross-talk reduction in a quantum-dot-based full-color micro-light-emitting-diode display by a lithographic-fabricated photoresist mold. *Photon. Res.* **2017**, *5* (5), 411−416.
(56) Zhang, X.; Qi, L.; Chong, W. C.; Li, P.; Tang, C. W.; Lau, K. M. Active matrix monolithic micro-LED full-color micro-display. *J. Soc. Inf. Display.* **2021**, *29* (1), 47−56.
(57) Chen, G.-S.; Wei, B.-Y.; Lee, C.-T.; Lee, H.-Y. Monolithic red/green/blue micro-LEDs with HBR and DBR structures. *IEEE Photonics Technol. Lett.* **2018**, *30* (3), 262−265.
(58) Hsiang, E.-L.; Li, Y.; He, Z.; Zhan, T.; Zhang, C.; Lan, Y.-F.; Dong, Y.; Wu, S.-T. Enhancing the efficiency of color conversion Micro-LED display with a patterned cholesteric liquid crystal polymer film. *Nanomaterials* **2020**, *10* (12), 2430.
(59) Chu, S.-Y.; Wang, H.-Y.; Lee, C.-T.; Lee, H.-Y.; Laing, K.-L.; Kuo, W.-H.; Fang, Y.-H.; Lin, C.-C. Improved color purity of monolithic full color micro-LEDs using distributed Bragg reflector and blue light absorption material. *Coatings* **2020**, *10* (5), 436.
(60) Theobald, D.; Yu, S.; Gomard, G.; Lemmer, U. Design of Selective Reflectors Utilizing Multiple Scattering by Core−Shell Nanoparticles for Color Conversion Films. *ACS Photonics* **2020**, *7* (6), 1452−1460.
(61) Chen, J.; Theobald, D.; Shams, A. B.; Jin, Q.; Mertens, A.; Gomard, G.; Lemmer, U. Silver-Nanoparticle-Based Metallodielectric Wavelength-Selective Reflectors for Quantum-Dot-Enhanced White-Light-Emitting Diodes. *ACS Appl. Nano Mater.* **2022**, *5* (1), 87−93.
(62) Gao, H.; Xie, Y.; Geng, C.; Xu, S.; Bi, W. Efficiency Enhancement of Quantum-Dot-Converted LEDs by 0D−2D Hybrid Scatterers. *ACS Photonics* **2020**, *7* (12), 3430−3439.
(63) Xu, S.; Yang, T.; Lin, J.; Shen, Q.; Li, J.; Ye, Y.; Wang, L.; Zhou, X.; Chen, E.; Ye, Y.; Guo, T. Precise theoretical model for quantum-dot color conversion. *Opt. Express* **2021**, *29* (12), 18654−18668.
(64) Tang, Y.; Li, Z.; Li, Z.; Li, J.; Yu, S.; Rao, L. Enhancement of Luminous Efficiency and Uniformity of CCT for Quantum Dot-Converted LEDs by Incorporating With ZnO Nanoparticles. *IEEE Trans. Electron Dev.* **2018**, *65* (1), 158−164.
(65) Yuce, H.; Guner, T.; Balci, S.; Demir, M. M. Phosphor-based white LED by various glassy particles: control over luminous efficiency. *Opt. Lett.* **2019**, *44* (3), 479−482.
(66) Yu, S.; Fritz, B.; Johnsen, S.; Busko, D.; Richards, B. S.; Hippler, M.; Wiegand, G.; Tang, Y.; Li, Z.; Lemmer, U.; Hölscher, H.; Gomard, G. Enhanced Photoluminescence in Quantum Dots−Porous Polymer Hybrid Films Fabricated by Microcellular Foaming. *Adv. Opt. Mater.* **2019**, *7* (12), 1900223.
(67) Li, J.-S.; Tang, Y.; Li, Z.-T.; Li, J.-X.; Ding, X.-R.; Yu, B.-H.; Yu, S.-D.; Ou, J.-Z.; Kuo, H.-C. Toward 200 Lumens per Watt of Quantum-Dot White-Light-Emitting Diodes by Reducing Reabsorption Loss. *ACS Nano* **2021**, *15* (1), 550−562.
(68) Hyun, B.-R.; Sher, C.-W.; Chang, Y.-W.; Lin, Y.; Liu, Z.; Kuo, H.-C. Dual Role of Quantum Dots as Color Conversion Layer and Suppression of Input Light for Full-Color Micro-LED Displays. *J. Phys. Chem. Lett.* **2021**, *12* (29), 6946−6954.
(69) Lin, C.-c.; Liang, K.-L.; Kuo, W.-H.; Shen, H.-T.; Wu, C.-I.; Fang, Y.-H. Colloidal Quantum Dot Enhanced Color Conversion Layer for Micro LEDs. *IEICE Trans. Electron.* **2022**, *E105.C*, 52−58.
(70) Chen, S.-W. H.; Huang, Y.-M.; Singh, K. J.; Hsu, Y.-C.; Liou, F.-J.; Song, J.; Choi, J.; Lee, P.-T.; Lin, C.-C.; Chen, Z.; Han, J.; Wu, T.; Kuo, H.-C. Full-color micro-LED display with high color stability using semipolar (20−21) InGaN LEDs and quantum-dot photoresist. *Photon. Res.* **2020**, *8* (5), 630−636.
(71) Liang, K.-L.; Kuo, W.-H.; Shen, H.-T.; Yu, P.-W.; Fang, Y.-H.; Lin, C.-C. Advances in color-converted micro-LED arrays. *Jpn. J. Appl. Phys.* **2020**, *60*, SA0802.
(72) Gou, F.; Hsiang, E.-L.; Tan, G.; Lan, Y.-F.; Tsai, C.-Y.; Wu, S.-T. Tripling the Optical Efficiency of Color-Converted Micro-LED Displays with Funnel-Tube Array. *Crystals* **2019**, *9* (1), 39.
(73) Zhou, Q.; Bai, Z.; Lu, W.-g.; Wang, Y.; Zou, B.; Zhong, H. In Situ Fabrication of Halide Perovskite Nanocrystal-Embedded Polymer Composite Films with Enhanced Photoluminescence for Display Backlights. *Adv. Mater.* **2016**, *28* (41), 9163−9168.
(74) Chang, S.; Bai, Z.; Zhong, H. In Situ Fabricated Perovskite Nanocrystals: A Revolution in Optical Materials. *Adv. Opt. Mater.* **2018**, *6* (18), 1800380.
(75) He, J.; Chen, H.; Chen, H.; Wang, Y.; Wu, S.-T.; Dong, Y. Hybrid downconverters with green perovskite-polymer composite films for wide color gamut displays. *Opt. Express* **2017**, *25* (11), 12915−12925.
(76) Wang, Y.; He, J.; Chen, H.; Chen, J.; Zhu, R.; Ma, P.; Towers, A.; Lin, Y.; Gesquiere, A. J.; Wu, S.-T.; Dong, Y. Ultrastable, Highly Luminescent Organic−Inorganic Perovskite−Polymer Composite Films. *Adv. Mater.* **2016**, *28* (48), 10710−10717.
(77) He, J.; Towers, A.; Wang, Y.; Yuan, P.; Jiang, Z.; Chen, J.; Gesquiere, A. J.; Wu, S.-T.; Dong, Y. In situ synthesis and macroscale alignment of CsPbBr3 perovskite nanorods in a polymer matrix. *Nanoscale* **2018**, *10* (33), 15436−15441.
(78) He, J.; He, Z.; Towers, A.; Zhan, T.; Chen, H.; Zhou, L.; Zhang, C.; Chen, R.; Sun, T.; Gesquiere, A. J.; Wu, S.-T.; Dong, Y. Ligand assisted swelling−deswelling microencapsulation (LASDM) for stable, color tunable perovskite−polymer composites. *Nanoscale Adv.* **2020**, *2* (5), 2034−2043.
(79) Zhang, C.; He, Z.; Chen, H.; Zhou, L.; Tan, G.; Wu, S.-T.; Dong, Y. Light diffusing, down-converting perovskite-on-polymer microspheres. *J. Mater. Chem. C* **2019**, *7* (22), 6527−6533.
(80) Zhang, C.; He, Z.; Mogensen, M.; Gesquiere, A. J.; Chen, C.-H.; Chiu, T.-L.; Lee, J.-H.; Wu, S.-T.; Dong, Y. A deep-dyeing strategy for ultra-stable, brightly luminescent perovskite-polymer composites. *J. Mater. Chem. C* **2021**, *9* (10), 3396−3402.
(81) Shi, L.; Meng, L.; Jiang, F.; Ge, Y.; Li, F.; Wu, X.-g.; Zhong, H. In Situ Inkjet Printing Strategy for Fabricating Perovskite Quantum Dot Patterns. *Adv. Funct. Mater.* **2019**, *29* (37), 1903648.

(82) Jia, S.; Li, G.; Liu, P.; Cai, R.; Tang, H.; Xu, B.; Wang, Z.; Wu, Z.; Wang, K.; Sun, X. W. Highly Luminescent and Stable Green Quasi-2D Perovskite-Embedded Polymer Sheets by Inkjet Printing. *Adv. Funct. Mater.* **2020**, *30* (24), 1910817.
(83) Fan, Q.; Biesold-McGee, G. V.; Ma, J.; Xu, Q.; Pan, S.; Peng, J.; Lin, Z. Lead-Free Halide Perovskite Nanocrystals: Crystal Structures, Synthesis, Stabilities, and Optical Properties. *Angew. Chem., Int. Ed.* **2020**, *59* (3), 1030−1046.
(84) Zhang, F.; Ma, Z.; Shi, Z.; Chen, X.; Wu, D.; Li, X.; Shan, C. Recent Advances and Opportunities of Lead-Free Perovskite Nanocrystal for Optoelectronic Application. *Energy Mater. Adv.* **2021**, *2021*, 5198145.
(85) Kim, S.; Lee, J.; Shin, M.; Kim, H.; Kim, Y. Integration of Prism Sheet on Quantum Dot Film With Bridge Patterns to Enhance Luminance of LED Backlight Unit. *IEEE Trans. Electron Devices* **2017**, *64* (3), 1153−1160.
(86) Lee, H.; Kim, Y. H.; Lim, Y. W.; Jang, J.; Kang, S. M.; Bae, B. S. Flexible but mechanically robust hazy quantum dot/glass fiber reinforced film for efficiently luminescent surface light source. *Adv. Opt. Mater.* **2020**, *8* (10), 1902178.
(87) Ji, H.; Xu, H.; Guo, J.; Yang, Y.; Zha, G. 28.2: Invited Paper: A new generation of QD Diffusion Plate Technology for TV. *SID Int. Symp. Dig Tec* **2021**, *52* (S1), 179−181.
(88) Tangirala, R.; Lee, E.; Sunderland, C.; Guo, W.; Mamuye, A.; Wang, K.; Hwang, E.; Kim, N.; Hotz, C. 62−7: Invited Paper: Quantum Dot Color Conversion for OLED and microLED Displays. *SID Int. Symp. Dig Tec* **2021**, *52* (1), 906−908.
(89) Lee, E.; Wang, C.; Hotz, C.; Hartlove, J.; Yurek, J.; Daniels, H.; Luo, Z.; Zehnder, D. 41−1: Invited Paper: "Greener" Quantum-Dot Enabled LCDs with BT.2020 Color Gamut. *SID Int. Symp. Dig Tec* **2016**, *47* (1), 549−551.
(90) Osinski, J.; Palomaki, P. In *4−5: Quantum Dot Design Criteria for Color Conversion in MicroLED Displays*; SID Int. Symp. Dig Tec. Wiley Online Library: 2019; pp 34−37.
(91) Gu, Z.; Wang, K.; Li, H.; Gao, M.; Li, L.; Kuang, M.; Zhao, Y. S.; Li, M.; Song, Y. Direct-Writing Multifunctional Perovskite Single Crystal Arrays by Inkjet Printing. *Small* **2017**, *13* (8), 1603217.
(92) Zou, C.; Chang, C.; Sun, D.; Böhringer, K. F.; Lin, L. Y. Photolithographic patterning of perovskite thin films for multicolor display applications. *Nano Lett.* **2020**, *20* (5), 3710−3717.
(93) Dai, X.; Zhang, Z.; Jin, Y.; Niu, Y.; Cao, H.; Liang, X.; Chen, L.; Wang, J.; Peng, X. Solution-processed, high-performance light-emitting diodes based on quantum dots. *Nature* **2014**, *515* (7525), 96−99.
(94) Dong, Y.; Caruge, J.-M.; Zhou, Z.; Hamilton, C.; Popovic, Z.; Ho, J.; Stevenson, M.; Liu, G.; Bulovic, V.; Bawendi, M.; Kazlas, P. T.; Steckel, J.; Coe-Sullivan, S. 20.2: Ultra-Bright, Highly Efficient, Low Roll-Off Inverted Quantum-Dot Light Emitting Devices (QLEDs). *SID Int. Symp. Dig Tec* **2015**, *46* (1), 270−273.
(95) Wang, L.; Lin, J.; Hu, Y.; Guo, X.; Lv, Y.; Tang, Z.; Zhao, J.; Fan, Y.; Zhang, N.; Wang, Y.; Liu, X. Blue Quantum Dot Light-Emitting Diodes with High Electroluminescent Efficiency. *ACS Appl. Mater. Interfaces* **2017**, *9* (44), 38755−38760.
(96) Li, X.; Lin, Q.; Song, J.; Shen, H.; Zhang, H.; Li, L. S.; Li, X.; Du, Z. Quantum-Dot Light-Emitting Diodes for Outdoor Displays with High Stability at High Brightness. *Adv. Optical Mater.* **2020**, *8* (2), 1901145.
(97) Cao, W.; Xiang, C.; Yang, Y.; Chen, Q.; Chen, L.; Yan, X.; Qian, L. Highly stable QLEDs with improved hole injection via quantum dot structure tailoring. *Nat. Commun.* **2018**, *9* (1), 2608.
(98) Pu, C.; Dai, X.; Shu, Y.; Zhu, M.; Deng, Y.; Jin, Y.; Peng, X. Electrochemically-stable ligands bridge the photoluminescence-electroluminescence gap of quantum dots. *Nat. Commun.* **2020**, *11* (1), 937.
(99) Shen, H.; Gao, Q.; Zhang, Y.; Lin, Y.; Lin, Q.; Li, Z.; Chen, L.; Zeng, Z.; Li, X.; Jia, Y.; Wang, S.; Du, Z.; Li, L. S.; Zhang, Z. Visible quantum dot light-emitting diodes with simultaneous high brightness and efficiency. *Nat. Photonics* **2019**, *13* (3), 192−197.
(100) Moon, H.; Lee, W.; Kim, J.; Lee, D.; Cha, S.; Shin, S.; Chae, H. Composition-tailored ZnMgO nanoparticles for electron transport layers of highly efficient and bright InP-based quantum dot light emitting diodes. *Chem. Commun.* **2019**, *55* (88), 13299−13302.
(101) Huang, Y.-Y.; Mroz, P.; Hamblin, M. R. Basic Photomedicine, 2009. http://photobiology.info/Photomed.html.
(102) Huang, Y.; Hamblin, M. *Handbook of Photomedicine*; CRC Press, Taylor & Francis: Boca Raton, 2013.
(103) Murawski, C.; Gather, M. C. Emerging Biomedical Applications of Organic Light-Emitting Diodes. *Adv. Optical Mater.* **2021**, *9* (14), 2100269.
(104) Triana, M. A.; Chen, H.; Zhang, D.; Camargo, R. J.; Zhai, T.; Duhm, S.; Dong, Y. Bright inverted quantum-dot light-emitting diodes by all-solution processing. *J. Mater. Chem. C* **2018**, *6* (28), 7487−7492.
(105) Chen, H.; He, Z.; Zhang, D.; Zhang, C.; Ding, Y.; Tetard, L.; Wu, S.-T.; Dong, Y. Bright Quantum Dot Light-Emitting Diodes Enabled by Imprinted Speckle Image Holography Nanostructures. *J. Phys. Chem. Lett.* **2019**, *10* (9), 2196−2201.
(106) Triana, M. A.; Wu, S.-T.; Dong, Y. P-105: Bright, Large Pixel, Flexible Quantum-Dot Light-Emitting Diodes for Photomedicine. *SID Int. Symp. Dig Tec* **2020**, *51* (1), 1748−1751.
(107) Triana, M. A.; El Hamid, H.; Celli, J.; Lanzafame, R.; Wu, S.-T.; Dong, Y. Quantum Dot Light-Emitting Diode Based Photomedicine: In Vitro Results to Date and Tunable Features for Targeted Phototherapy. *Proc. 28th Int. Display Workshops* **2021**, *28*, 810−813.
(108) van de Weijer, P.; Bouten, P. C. P.; Unnikrishnan, S.; Akkerman, H. B.; Michels, J. J.; van Mol, T. M. B. High-performance thin-film encapsulation for organic light-emitting diodes. *Org. Electron.* **2017**, *44*, 94−98.
(109) Ding, K.; Fang, Y.; Dong, S.; Chen, H.; Luo, B.; Jiang, K.; Gu, H.; Fan, L.; Liu, S.; Hu, B.; Wang, L. 24.1% External Quantum Efficiency of Flexible Quantum Dot Light-Emitting Diodes by Light Extraction of Silver Nanowire Transparent Electrodes. *Adv. Opt. Mater.* **2018**, *6* (19), 1800347.
(110) Yu, R.; Wang, T.; Kang, Z.; Zhang, H.; Zhang, H.; Ji, W. Intaglio-type random silver networks as the cathodes for efficient full-solution processed flexible quantum-dot light-emitting diodes. *Nanoscale* **2018**, *10* (47), 22541−22548.
(111) Hamblin, M. *Advances in photodynamic therapy: basic, translational, and clinical*; Artech House: Norwood, MA, 2008.
(112) Cieplik, F.; Deng, D.; Crielaard, W.; Buchalla, W.; Hellwig, E.; Al-Ahmad, A.; Maisch, T. Antimicrobial photodynamic therapy − what we know and what we don't. *Crit. Rev. Microbiol.* **2018**, *44* (5), 571−589.
(113) Tuner, J.; Hode, L. *The new laser therapy Handbook: a guide for research scientists, doctors, dentists, veterinarians and other interested parties within the medical field*; Prima Books AB, 2010.
(114) Avci, P.; Gupta, A.; Sadasivam, M.; Vecchio, D.; Pam, Z.; Pam, N.; Hamblin, M. R. *Low-level laser (light) therapy (LLLT) in skin: stimulating, healing, restoring*, Seminars in cutaneous medicine and surgery; NIH Public Access: 2013; p 41.
(115) Myakishev-Rempel, M.; Stadler, I.; Polesskaya, O.; Motiwala, A. S.; Nardia, F. B.; Mintz, B.; Baranova, A.; Zavislan, J.; Lanzafame, R. J. Red Light Modulates Ultraviolet-Induced Gene Expression in the Epidermis of Hairless Mice. *Photomed Laser Surg.* **2015**, *33* (10), 498−503.
(116) J, L. R., The recalcitrant wound: using low-level light therapy to manage non-healing wounds and ulcers. In *Handbook of low-level laser therapy*; Hamblin, M. R., Agrawal, T., de Sousa, M.,, Eds.; Jenny Stanford Publishing: New York, 2017; pp 581−596.
(117) Turrens, J. F. Mitochondrial formation of reactive oxygen species. *J. Physiol.* **2003**, *552*, 335−344.
(118) Lanzafame, R.; Stadler, I.; Dong, Y.; Chen, H.; Wu, S.-T.; He, J. Preliminary Studies of a Novel Red-Emitting Quantum Dot Led Source for Photobiomodulation Applications. *Lasers Surg. Med.* **2017**, *49*, 57−58.
(119) Lanzafame, R. J.; Stadler, I.; Dong, Y.; Chen, H.; He, J.; Blackman, J.; Pennino, R. P. Preliminary Studies of a Novel Red-

Emitting Quantum Dot Led Source for Photobiomodulation for In Vitro Model of the Wound Healing. *Lasers Surg. Med.* **2018**, *50*, 359−360.
(120) Kim, T.-H.; Lee, C.-S.; Kim, S.; Hur, J.; Lee, S.; Shin, K. W.; Yoon, Y.-Z.; Choi, M. K.; Yang, J.; Kim, D.-H.; et al. Fully stretchable optoelectronic sensors based on colloidal quantum dots for sensing photoplethysmographic signals. *ACS Nano* **2017**, *11* (6), 5992−6003.
(121) Kim, J.; Shim, H. J.; Yang, J.; Choi, M. K.; Kim, D. C.; Kim, J.; Hyeon, T.; Kim, D.-H. Ultrathin Quantum Dot Display Integrated with Wearable Electronics. *Adv. Mater.* **2017**, *29* (38), 1700217.
(122) Jeon, Y.; Choi, H.-R.; Kwon, J. H.; Choi, S.; Nam, K. M.; Park, K.-C.; Choi, K. C. Sandwich-structure transferable free-form OLEDs for wearable and disposable skin wound photomedicine. *Light Sci. Appl.* **2019**, *8* (1), 114.
(123) Choi, M. K.; Yang, J.; Hyeon, T.; Kim, D.-H. Flexible quantum dot light-emitting diodes for next-generation displays. *npj Flex. Electron* **2018**, *2* (1), 10.
(124) Lee, Y.; Kim, D.-H. Wireless metronomic photodynamic therapy. *Nat. Biomed. Eng.* **2019**, *3* (1), 5−6.
(125) Kim, S. H.; Baek, G. W.; Yoon, J.; Seo, S.; Park, J.; Hahm, D.; Chang, J. H.; Seong, D.; Seo, H.; Oh, S.; et al. Stretchable Sensory-Neuromorphic System. *Adv. Mater.* **2021**, *33*, 2104690.
(126) Mao, D.; Xiong, Z.; Donnelly, M.; Xu, G. Brushing-Assisted Two-Color Quantum-Dot Micro-LED Array Towards Bi-Directional Optogenetics. *IEEE Electron Device Lett.* **2021**, *42* (10), 1504−1507.

https://doi.org/10.1021/acsenergylett.1c02745
ACS Energy Lett. 2022, 7, 1001−1020